sustainability

MDPI

Article

Synergistic Optimization of Mortar Performance and Carbon Footprint Reduction Using Quarry Wastes and Natural Pozzolana: A Statistical and Experimental Study

Abdellah Douadi [1,2], Ali Makhlouf [3], Cherif Belebchouche [1,2,*], Kamel Hebbache [1,2], Mourad Boutlikht [1], Laura Moretti [4], Paulina Faria [5], Hammoudi Abderazek [6,7], Sławomir Czarnecki [8,*] and Adrian Chajec [8]

1 Civil Engineering Research Laboratory of Setif (LRGCS), Department of Civil Engineering, Setif 1 University-Ferhat Abbas, Setif 19000, Algeria; abdellah.douadi@univ-setif.dz (A.D.); hebbache.kamel@univ-setif.dz (K.H.); mouradboutlikht@gmail.com (M.B.)
2 Emergent Materials Research Unit (URME), Department of Civil Engineering, Setif 1 University-Ferhat Abbas, Setif 19000, Algeria
3 Geological Sciences Department, FSBSA, Mouloud MAMMERI University of Tizi-Ouzou, PB N° 17 RP, Tizi Ouzou 15000, Algeria; ali.makhlouf@ummto.dz
4 Department of Civil, Constructional and Environmental Engineering, Sapienza University of Rome, Via Eudossiana 18, 00184 Rome, Italy; laura.moretti@uniroma1.it
5 Civil Engineering Research and Innovation for Sustainability, Department of Civil Engineering, NOVA School of Science and Technology, NOVA University Lisbon, 2829-516 Caparica, Portugal; paulina.faria@fct.unl.pt
6 UR-MPE, M'hamed Bougara University, Independence Avenue, Boumerdes 35000, Algeria
7 Applied Precision Mechanics Laboratory, Institute of Optics and Precision Mechanics, Setif 1 University-Ferhat Abbas, Setif 19000, Algeria
8 Department of Materials Engineering and Construction Processes, Wroclaw University of Science and Technology, 50-370 Wroclaw, Poland; adrian.chajec@pwr.edu.pl
* Correspondence: cherif.belebchouche@univ-setif.dz (C.B.); slawomir.czarnecki@pwr.edu.pl (S.C.)

Abstract

The construction industry increasingly integrates technological advancements to enhance efficiency and meet technical, environmental, and economic requirements. Self-compacting mortars are gaining popularity due to their superior fluidity, optimized compaction, and improved mechanical properties. This study explores the potential of statistical mix design methodology to optimize self-compacting mortars' fresh properties and strength development by replacing up to 20% of cement with pozzolana, limestone, and marble powder. A self-compacting mortar repository was used to develop robust models predicting slump flow, compressive strength at 28 days, water absorption, and capillary absorption. Results indicate that marble powder mixtures exhibit superior slump flow, up to 9% higher than other formulations. Compressive strengths range from 50 MPa to 70 MPa. Pozzolana and marble-based mortars show 15% and 12% strength reductions compared to the limestone-based mix, respectively. Water absorption increases slightly for mortars with marble (+2%) or pozzolana (+3%). The mortar containing marble powder has the lowest sorptivity coefficient due to its high specific surface area. The statistical analysis was conducted using a mixture design approach based on a second-order polynomial regression model. ANOVA results for the studied responses indicate that the calculated F-values exceed the critical thresholds, with *p*-values below 0.05 and R-squared values above 0.83, confirming the robustness and predictive reliability of the developed models. Life cycle assessment reveals that cement production accounts for over 80% of the environmental impact. Partial replacement with pozzolana, limestone, and marble powder reduces up to 19% of greenhouse gas emissions and 17.22% in non-renewable energy consumption, demonstrating the environmental benefits of optimized formulations.

Academic Editor: Antonio Caggiano

Received: 17 July 2025
Revised: 8 August 2025
Accepted: 9 August 2025
Published: 14 August 2025

Citation: Douadi, A.; Makhlouf, A.; Belebchouche, C.; Hebbache, K.; Boutlikht, M.; Moretti, L.; Faria, P.; Abderazek, H.; Czarnecki, S.; Chajec, A. Synergistic Optimization of Mortar Performance and Carbon Footprint Reduction Using Quarry Wastes and Natural Pozzolana: A Statistical and Experimental Study. *Sustainability* **2025**, *17*, 7346. https://doi.org/10.3390/su17167346

Keywords: self-compacting mortar; mechanical properties; ANOVA; optimization; life cycle assessment

1. Introduction

Despite the efforts made by cement-producing companies to reduce CO_2 emissions, the chemical and thermal processes involved in cement production still account for about 8% of global greenhouse gas emissions [1,2]. As a result, researchers have been exploring environmentally friendly raw materials to create alternative binders for cement in an attempt to lower these emissions [3–5].

Ensuring the sustainable use of natural resources in the face of rapid global population growth is one of the most pressing issues facing humanity today [6]. Simultaneously, the problem of disposing of industrial waste and by-products is worsening, as landfills pose a threat to human health as well as the stability of the natural environment [7]. By using waste and industrial by-products as secondary raw materials, the construction industry is moving towards a more circular economic model in this regard [8]. This approach addresses the waste disposal issue while also reducing raw material consumption in construction.

At the front of this sustainable change are self-compacting mortars (SCMs). Their capacity to flow and consolidate under their own weight without the need for mechanical vibration [9], thus reducing energy, equipment and man power consumption This remarkable property is due to their inherent fluidity and stability. The incorporation of fillers, derived either from industrial or quarries waste, such as crushed bricks [10], other ceramic debris [11], marble powder [12], glass powder [13] and limestone filler [14], or natural resources such as, dune sand and volcanic tuffs [15,16], plays a critical role in enhancing the physico-mechanical properties of SCMs. These fillers, in optimized percentages, due to their fine particle size and ability to fill voids between cement grains, improve the compactness, mechanical strength, and durability of the mortars [17].

This enhances the homogeneity and stability of fresh self-compacting mortars (SCMs), reducing segregation and bleeding risks. Fillers significantly reduce clinker demand in cement production, thereby lowering the carbon footprint of the final product. For instance, CEM II/A and CEM II/B cements contain approximately 80–94% and 65–79% clinker, respectively, while CEM III/A, B, and C cements contain as little as 35–64%, 20–34%, and 5–19% clinker, respectively, due to the incorporation of supplementary materials such as slag or fillers. This reduction in clinker content contributes directly to lower CO_2 emissions associated with calcination and fuel combustion during cement production.

Studies have shown that substituting 15–30% of Portland cement with inert filler such as limestone, brick powder, or ceramic waste can decrease CO_2 emissions by up to 200–300 kg per ton of cement produced [18,19], depending on the substitution level and process efficiency. In mortar and concrete formulations, the incorporation of such fillers also reduces overall cement consumption without compromising mechanical properties when properly optimized [20].

Fillers also lower clinker demand in cement production, reducing its carbon footprint, and cement consumption in mortars and concrete. Industrial by-products, such as brick powder, ceramic waste, and construction demolition residues, offer promising opportunities for reducing clinker consumption, minimizing landfill disposal, and promoting circular economy principles. These materials can act as fillers or exhibit latent hydraulic or pozzolanic properties when finely ground, contributing to improved mechanical performance and lower environmental impact. However, their large-scale application may face certain limitations, including inconsistent availability, regional disparities in source quality, and the

need for preprocessing (e.g., crushing, grinding, and sieving) to achieve appropriate fineness and chemical compatibility with cementitious systems. In some cases, contaminants such as sulfates, alkalis, or organic matter may also restrict their reuse without adequate treatment. Addressing these challenges through standardization protocols, quality control, and local valorization strategies is essential to ensure their safe, reliable, and scalable integration into sustainable construction materials [21,22].

Dune sand, limestone powder, and marble powder offer distinct benefits. Finely ground dune sand provides a sustainable use for this abundant local resource, though salt contamination must be considered [23]. However, a critical limitation of dune sand is its potential contamination by chlorides and sulfates, originating from windborne marine aerosols or groundwater salinity. These salts can adversely affect cement hydration, promote corrosion of embedded reinforcement, and compromise long-term durability of concrete.

Despite this, dune sand remains a viable SCM option, particularly when appropriate pretreatment strategies are implemented. These include washing with freshwater, thermal treatment, or blending with low-salt aggregates to reduce soluble salt content to within acceptable limits defined by standards (e.g., ASTM C33 or EN 12620). Moreover, when used in finely ground form, dune sand exhibits pozzolanic reactivity and filler effects that contribute to improved particle packing and mechanical properties. With controlled processing, its environmental and economic advantages justify its use in eco-efficient binder systems, especially in regions where natural resources are constrained. Limestone filler, widely used in cement-based materials, improves SCM workability and stability [24]. Marble powder, a by-product of marble processing, is rich in calcium carbonate and retains natural marble's chemical stability and whiteness. Its fine particle size enhances the mechanical properties, workability, and surface finish of mortars and concrete [25]. Incorporating marble powder supports industrial waste recycling while improving SCM performance, contributing to sustainable construction through waste valorization and efficient resource utilization [26].

This dual approach of innovation and sustainability paves the way for a new generation of construction materials that combine high performance with environmental responsibility. By integrating these advanced materials, the construction industry can achieve significant economic and ecological benefits, contributing to the development of more sustainable building practices [27]. Several studies have explored the incorporation of limestone powder (LSP) as a sole supplementary cementitious material (SCM) in cementitious systems [28–30], while only a limited number have investigated the combined use of multiple SCMs, particularly ternary blends involving pozzolana (PZ) [31–33]. The isolated use of these materials may not yield optimal performance, especially in self-compacting concretes (SCCs) [34]. For instance, LSP alone tends to increase the demand for high-range water-reducing admixtures (HRWRAs) to achieve the required flowability while also inducing significant early-age dimensional instability due to shrinkage effects [34]. Further investigations by Belaidi et al. [35], examined the influence of marble powder (MP) and pozzolana (PZ) on the rheological and mechanical properties of SCCs. The findings indicate that PZ contributes to enhanced long-term strength development in binary systems, particularly at 90 days. The highest compressive strength at 28 days was recorded in mixtures incorporating 5% PZ in binary systems and a ternary blend of 5% PZ + 5% MP, demonstrating the potential of these optimized formulations to improve both fresh and hardened properties of SCCs.

Traditional mix design methods may not adequately address the strict requirements of self-compacting mortars (SCMs). Data-driven approaches offer valuable insights for optimizing fresh properties while improving strength development [36]. The Design of

Experiments (DoE) is a powerful statistical tool that helps establish correlations between variables, identify optimal responses, minimize experimental trials, and create mathematical models based on predefined inputs [37]. In recent decades, statistical methods have become increasingly important in the design of mortar and concrete mixes. Researchers have utilized experimental design techniques to maximize material substitution, incorporating alternatives such as pumice stone [38], foundry sand [39], plastic waste [40], silica fume [41], and hybrid steel fibers [42] to replace cement or aggregates. These studies have resulted in high-precision models that optimize cementitious mixes while reducing the consumption of primary raw materials [43–45]. To optimize mix designs, researchers can systematically adjust substitution rates and analyze their effects, balancing performance with environmental impact. This approach enhances sustainability by minimizing waste and resource depletion, leading to more efficient and eco-friendly construction materials [46].

In general, the incorporation of experimental design methodologies into the development of SCMs an important step in the pursuit of sustainable construction practices. This approaches enables to optimize the material properties, ensuring that self-compacting mortars meet modern construction standards while minimizing their environmental impact [47]. Through continued research and application of these statistical tools, the construction industry can achieve significant progress toward more sustainable and resilient infrastructure.

This research aims to compare the performance of limestone powder (LSP) and marble powder (MP) when combined with a pozzolanic addition, given that both materials are calcium-rich and traditionally considered inert fillers. The objective is to establish optimal mix designs that enhance self-compacting mortars' mechanical strength and durability (SCMs) by incorporating controlled proportions of LSP, MP, and pozzolana powder (PZ). Previous studies have demonstrated that including inert fillers can improve the overall performance of cementitious materials, with filler contents reaching up to 15% and pozzolana additions up to 5% [48–50]. However, a comprehensive understanding of synergistic effects arising from ternary blends remains limited. This study seeks to bridge this knowledge gap by systematically evaluating the influence of replacing up to 20% of cement with varied combinations of LSP, MP, and PZ, leveraging experimental design methodologies to optimize mixture formulations for enhanced workability, mechanical performance, and long-term durability

This study reveals important contributions to the field of sustainable construction materials development. It provides two major contributions:

(1) It proposes a systematic optimization framework for incorporating industrial by-products, such as limestone powder and marble powder, and natural pozzolanic resources into self-compacting mortars. This approach tackles issues related to waste management while meeting the construction industry's increasing demand for sustainable alternatives to conventional cementitious binders. Implementing a statistical mixture design approach facilitates a rigorous evaluation of multiple variables and their interactions within a ternary system of supplementary cementitious materials.

(2) The findings reveal that strategically incorporating these fillers enhances self-compacting mortars' mechanical and durability performance. The observed improvements in the studied responses provide robust experimental validation, reinforcing the viability of these materials for structural applications. This research establishes optimal mix proportions using a comprehensive statistical modeling approach, ensuring superior performance relative to conventional mortar formulations. This data-driven methodology offers precise guidance for material selection, quality control, and large-scale practical implementation.

(3) A life cycle assessment (LCA) was performed to quantify the environmental footprint of the developed mortars, particularly in terms of greenhouse gas emissions and

non-renewable energy consumption. The insights gained from this analysis underscore the potential of these optimized formulations to contribute to eco-efficient construction practices, aligning with global sustainability objectives.

2. Materials and Methods

2.1. Materials

Mortars were prepared using a CEM I 42.5 R Portland cement, as classified by EN 197-1 [51], produced by the Biskria cement company. This cement has a specific gravity of 3.15 g/cm^3 and a Blaine specific surface area of 326 m^2/kg. The sand used had a maximum grain size of 3.15 mm and a fineness modulus of 2.5. It was obtained by blending 30% of very fine natural siliceous sand with 70% of crushed artificial sand, in accordance with Abrams' rule, which in this context was applied to optimize the particle size distribution [52]. The natural sand had a fineness modulus of 0.937 and a sand equivalent value of 67.71%, whereas the crushed sand exhibited a fineness modulus of 3.167 and a sand equivalent of 83.67%.

Besides cement and sand, after reduced to powders, natural pozzolana from Beni Saf (P), limestone from The Khroub quarry (L) and marble powder from ZIDANE Mouloud Establishments, PLM were included as additives. The materials underwent intensive grinding using a laboratory-type Shredder A BB 27 for 60 min in the case of pozzolana and 90 min for limestone and marble before utilization. The chemical compositions of each additive, along with the used cement, are presented in Table 1. The relatively high loss on ignition (LOI) values recorded for marble (39.8%) and limestone (43.6%) are primarily due to the thermal decomposition of their carbonate constituents during heating. These materials are composed predominantly of calcium carbonate ($CaCO_3$), and in the case of some limestones, also dolomite ($CaMg(CO_3)_2$). When subjected to ignition temperatures (typically above 600 °C), $CaCO_3$ and dolomite decompose to form CaO and MgO, respectively, while releasing carbon dioxide (CO_2) gas according to the reactions:

$$CaCO_3 \rightarrow CaO + CO_2 \quad (1)$$

$$CaMg(CO_3)_2 \rightarrow CaO + MgO + 2CO_2 \quad (2)$$

Table 1. Chemical composition of cement, pozzolana, limestone and marble powders.

Compound (% wt.)	Cement	Pozzolana	Marble	Limestone
SiO_2	22.7	47.8	7.44	1
Al_2O_3	5.4	19.8	0.83	0.3
Fe_2O_3	2.7	10.5	0.75	0.3
CaO	65.7	9.2	49.73	53.3
MgO	0.7	3.8	0.66	1.1
SO_3	0.6	0.2	0.01	0.07
K_2O	0.4	0.5	0.02	0.04
Na_2O	0.7	0.8	0.01	0.06
Loss On Ignition L.O.I.	0.3	6.5	39.8	43.6
Specific gravity (g/cm^3)	3.15	3.13	3.24	3.18
Blaine specific surface (kg/m^2)	326	370	480	422

This release of gaseous CO_2 leads to a significant reduction in sample mass, which explains the elevated LOI values observed. These results confirm the high carbonate content of marble and limestone, characteristic of their calcareous origin.

2.2. Mortars and Specimens' Preparation

Since the presented experimental program attempts to discern the influence of pozzolana, limestone and marble powders on mortar characteristics, a mixture design was developed. This plan includes the three additives (*L*, *M*, and *P*) as factors expressed in mass proportions, where the sum is equal to the unit, used as cement replacements with an amount of 20%. This means that these factors are interdependent. The experimental field is constrained by Equation (3):

$$\sum_{i=1}^{i=n} = 1 \quad (3)$$

The number of necessary experiments to achieve the aim of this research is determined using Equation (4):

$$C_{q+m-1}^{m} = \frac{(q + m - 1)!}{(m!)(q - 1)!} \quad (4)$$

with q being the number of factors and m being the number of levels. Considering three factors and three levels, the influence of these factors on the properties of mortars can be predicted using a mortar design comprising 10 mixtures.

The quantities of all components used in the formulation of the predefined mortars are presented in Table 2. It is important to note that the binder-to-sand (B/S) ratio, the water-to-binder (W/B) ratio, and the superplasticizer dosage were maintained constant at 0.562%, 0.38%, and 1.5%, respectively, across all mortar formulations.

Table 2. Amounts of mixture components of studied self-compacting mortars.

Mortars	Main Components (kg/m^3)			Additives (kg/m^3)		
	Cement	Sand	Water	Pozzolana	Limestone Powder	Marble Powder
M 1 (1P)	564	1350	225	141	0	0
M 2 (1/3L2/3P)				93.07	46.53	0
M 3 (2/3L1/3P)				46.53	93.07	0
M 4 (1L)				0	141	0
M 5 (1/3M2/3P)				93.07	0	46.53
M 6 (1/3L1/3M1/3P)				46.53	46.53	46.53
M 7 (1/3M2/3L)				0	93.07	46.53
M 8 (2/3M1/3P)				46.53	0	93.07
M 9 (2/3M1/3L)				0	46.53	93.07
M 10 (1M)				0	0	141

Mortars were prepared in compliance with the recommendations of Okamura and Ozawa [53], which are based on achieving self-compactability through a proper balance of powder content, water-to-powder ratio, and superplasticizer dosage, without the need for vibration. Three specimens were tested for every mortar. The reported test results represent the average of the three measured values per mortar.

2.3. Experimental Program

Figure 1 presents the adopted experimental program and illustrates the strategy of the current study in investigating the behavior of SCMs containing pozzolana, limestone and marble powder.

The slump flow test for the SCMs was conducted following EFNARC guidelines and standards [54], which standardize the assessment of workability and flow characteristics. The Compressive strength was performed on three samples at 7 and 28 days in accordance

with EN 1015-11 [55]. The ultrasonic pulse velocity (UPV) of the cement paste was measured. The UPV value was calculated using the following equation:

$$V = \frac{h}{t} \times 10^6 \tag{5}$$

where V (m/s) is the ultrasonic pulse velocity, h (m) represents the distance between the transmitting and receiving surfaces of the cement-based specimen, and t (µs) denotes the time taken by the ultrasonic waves to travel between these surfaces.

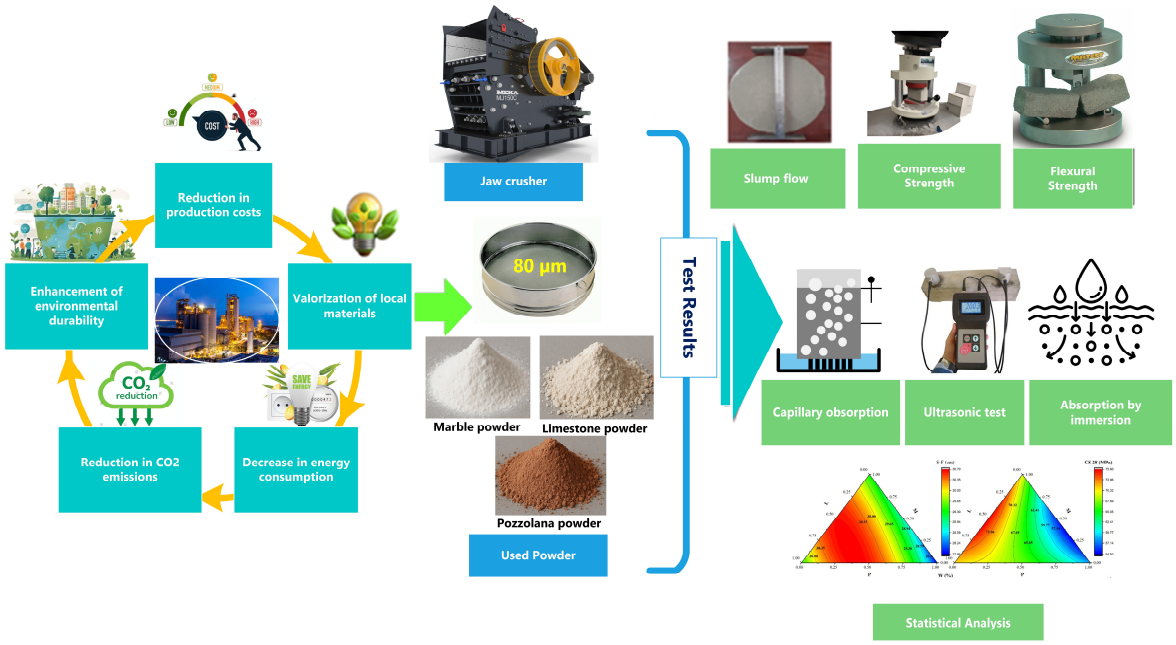

Figure 1. Adopted experimental program applied on self-compacting mortars containing pozzolana, limestone and marble powder.

The absorption by immersion test follows a straightforward procedure and requires no prior preparation, as specified in ASTM C1403 [56]. This test involves immersing mortar specimens in water at a controlled temperature of 20 ± 2 °C until a constant mass is achieved. The water absorption percentage is then calculated using Equation (6).

$$W(\%) = \frac{m_f - m_0}{m_0} \times 100 \tag{6}$$

where m_0 is the sample constant mass before immersion and m_f is its mass after immersion.

The capillary water absorption test was performed in accordance with ASTM C-1585 standards [54]. The capillary water absorption test was performed in accordance with ASTM C-1585 standards [51]. After immersion in water for 28 days, the mortar samples were thoroughly dried in an oven at 50 °C and 80% relative humidity. To ensure unidirectional water absorption, the lateral surfaces of the prismatic samples were then sealed with a layer of epoxy resin. The base of each sample was then placed in contact with water. The test duration is three days, with the first six hours being particularly critical and requiring close monitoring. The capillary curve of each mortar is drawn. The capillary absorption coefficient is calculated using Equation (7):

$$CA = \frac{m_f - m_0}{a^2 \times \sqrt{t}} \tag{7}$$

with *CA* being the capillary absorption coefficient, in (kg/m^2·min$^{1/2}$), m_f being the sample mass after a specified time of absorption, in (kg), m_0 being the initial mass of the dry sample, also in (kg), *a* being the surface area of the specimen in contact with water, in (m^2) and *t* being the absorption time, in (min).

In the assessment of mix design models, particularly within regression analysis, multiple performance indicators are utilized to rigorously evaluate the model's accuracy and reliability. Among these, the coefficient of determination (R^2) is a key statistical measure reflecting the model's predictive efficiency. This coefficient quantifies the extent to which the variability of the dependent variable is explained by the independent variables. An R^2 value approaching unity indicates a strong correlation between predicted and observed values, demonstrating the model's ability to capture most of the dataset's variance [57]. Another critical performance metric is the root mean square error (*RMSE*), which is particularly sensitive to substantial deviations. By assigning greater weight to larger errors, *RMSE* provides a direct estimation of the average prediction error magnitude, offering insight into the model's absolute predictive performance.

While R^2 indicates how well the model explains variance, it does not account for the scale of prediction errors. *RMSE* complements R^2 by quantifying the actual error size in the same units as the output variable, which is essential for practical interpretation and comparison across models. Therefore, the joint use of R^2 and *RMSE* ensures a balanced evaluation of both the model's explanatory power and its predictive accuracy [58].

Employing multiple performance criteria allows for a more holistic evaluation of predictive accuracy, facilitating a thorough comparison between model estimations and empirical data. Since each metric highlights different aspects of predictive performance, their combined use ensures a robust assessment framework. The fundamental equations for R^2 and *RMSE* are given as follows:

$$R^2 = 1 - \frac{\sum_{i=1}^{n}(P_z - O)}{\sum_{i=1}^{n}(P_z - Z)} \tag{8}$$

$$RMSE = \sqrt{\frac{1}{n}\sum_{i=1}^{n}(P_z - Z)} \tag{9}$$

where *n* is the number of observations, P_z is the value predicted by the model, *O* is the observed value, *z* is the average of the actual values.

An analysis of variance (ANOVA) was conducted to statistically evaluate the influence of the independent variables on the response metrics, with the aim of distinguishing systematic effects from random experimental error. The test employed the *F*-distribution, wherein the *F* ratio calculated as the ratio of the mean square of a given factor to the mean square of the residual is compared against a critical *F*-value at a 95% confidence level ($\alpha = 0.05$). The Fisher–Snedecor test was applied to assess the statistical relevance of each model term. The total degrees of freedom were partitioned into model-related components (including lack-of-fit), pure error (residual), and total system variability, denoted, respectively, as dof_1, dof_2, and dof_3, and formalized in Equations (10)–(12).

$$dof_1 = p - 1 \tag{10}$$

$$dof_2 = n - p \tag{11}$$

$$dof_3 = n - 1 \tag{12}$$

where *p* is the number of estimated coefficients and *n* is the number of training samples (10 and 14 in this study).

The desirability function, initially introduced by Derringer and Suich, is a widely utilized method for multi-response optimization, offering a systematic approach to reconciling multiple objectives in experimental design. This technique transforms each observed response (Y_i) into a corresponding desirability value ($d(Y_i)$) within a standardized scale ranging from 0 to 1, where 0 denotes an unsatisfactory outcome and 1 signifies the most favorable result. The overall desirability index (D) is subsequently determined as the geometric mean of individual desirability values, as formulated in Equation (13) [59]:

$$D = (d(Y\_1) \times d(Y\_2) \times \ldots \times d(Y\_i))\left(\frac{1}{n}\right) = \prod_{i=1}^{n} d(Y\_i)^{\left(\frac{1}{n}\right)} \quad (13)$$

where n represents the total number of responses. The primary objective of the optimization process is to maximize D by adjusting key input parameters (P, M, and L). The desirability function of each response is determined based on its target value or range. For instance, responses following a "greater is better" criterion are modeled using Equation (14), while those exhibiting a "smaller is better" trend are described by Equation (15) [60]:

$$d(Y\_i)max = \begin{cases} 0 & Y\_i < L\_i \\ \left(\frac{Y\_i - L\_i}{U\_i - L\_i}\right)^{r\_i} & L\_i \le Y\_i \le U\_i \\ 1 & Y\_i > U\_i \end{cases} \quad (14)$$

$$d(Y\_i)min = \begin{cases} 0 & Y\_i < L\_i \\ \left(\frac{U\_i - Y\_i}{U\_i - L\_i}\right)^{r\_i} & L\_i \le Y\_i \le U\_i \\ 1 & Y\_i > U\_i \end{cases} \quad (15)$$

where L_i and U_i correspond to the lower and upper limits for the ith response, respectively, and r_i is the assigned weighting factor, ensuring that $\sum r_i = 1$.

This optimization approach efficiently balances competing performance criteria, including the flow test, compressive strength at 28 days, ultrasonic pulse velocity (UPV), absorption by immersion, and capillary absorption, while accounting for their relative importance. The result is a single optimized solution that represents the best overall performance of the self-compacting mortars under study.

3. Results and Discussion

3.1. Flow of Self-Compacting Mortars

Figure 2 illustrates the slump flow results of the tested mortars, revealing clear trends in the influence of different powder additions. The corresponding coefficients of variation (CV), ranging from 1.05% to 3.72%, indicate a high degree of measurement consistency and reproducibility. Mortars with pozzolana exhibited lower flow values compared to those incorporating marble or limestone powders, highlighting the influence of pozzolana content on workability. Conversely, mortars containing marble powder—particularly those with 93.07 kg/m^3 of limestone and 46.53 kg/m^3 of marble powder but no pozzolana demonstrated the highest slump flow, suggesting enhanced fluidity in the absence of pozzolanic additives.

The mortar containing only pozzolana (M1) or only limestone (M10) showed a decrease in spread by 9% and 3%, respectively, when compared to the mortar containing only marble. Furthermore, mortars with higher marble content (M3 and M4) exhibited greater flow compared to M2 and M9, with respective increases of 5% and 3%, confirming the positive impact of marble powder on workability.

The corresponding coefficients of variation (CV), ranging from 1.05% to 3.72%, indicate a high degree of consistency and reproducibility in the measurements. Although a slight

increase in slump flow is observed among the different mortar compositions, the low CV values reflect minimal variability within replicates, thereby reinforcing the reliability of the experimental data. From a statistical perspective, such limited dispersion suggests that the observed differences in mean slump flow values likely lie within the bounds of experimental uncertainty. It can be seen that mortar mixtures containing pozzolana are characterized with lower flow in comparison to those where the other powders were added. In case of the samples where marble powder was added they are characterized with the highest slump flow in comparison to the samples where such additive was not applied. The highest slump was observed for the samples where the pozzolana was not added to the mixture but only 93.07 kg/m^3 of limestone powder and 46.53 kg/m^3 of marble powder. The mortar containing only pozzolana (M1) or limestone (M10) showed a decrease in spread by 9% and 3%, respectively, compared to the mortar containing only marble. Mortars with a higher proportion of marble, namely M3 and M4, exhibited greater flow compared to mortars M2 and M9, with respective increases of 5% and 3%.

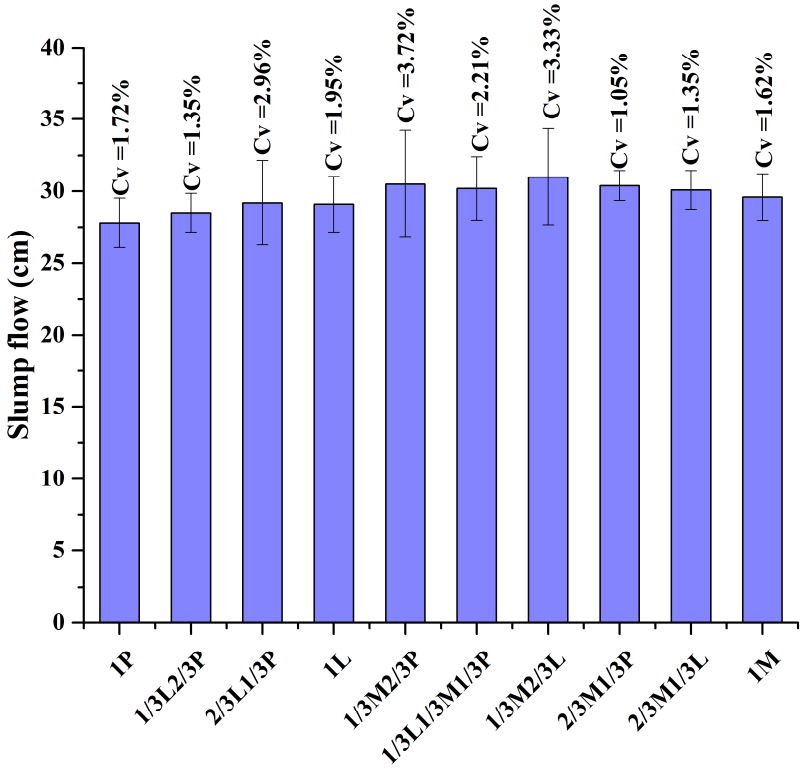

Figure 2. Slump flow of mortars.

3.2. Compressive Strength

Figure 3 presents the compressive strength evolution of the studied mortars at 7 and 28 days. At 7 days, mortars M4 (containing marble) and M1 (containing pozzolana) exhibit a reduction in compressive strength compared to M10 (containing only limestone), with decreases of approximately 6% and 4%, respectively. This behavior can be explained by considering the specific surface area (Blaine specific surface, BSS) of the powders used. While marble and pozzolana exhibit higher fineness (480 m^2/kg and 370 m^2/kg, respectively) than cement (326 m^2/kg), their isolated incorporation may lead to dilution of the cementitious phase without sufficient early-age reactivity, especially for pozzolana whose pozzolanic reaction is slow. Limestone powder (BSS = 422 m^2/kg), on the other hand, contributes effectively at early ages through physical effects (filler and nucleation), improving the packing density and promoting the hydration of clinker phases [61,62].

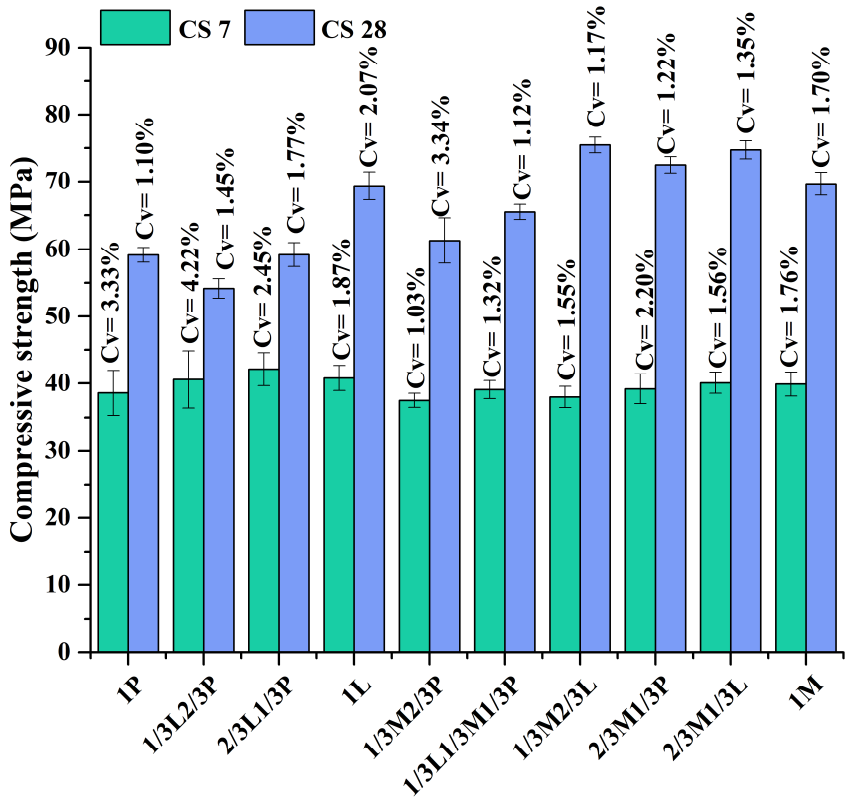

Figure 3. Compressive strength of mortars at 7 days and 28 days.

In contrast, binary mortars (e.g., M2, M3, M5), combining limestone, marble, and/or pozzolana, show enhanced compressive strengths at 7 days compared to single-additive mortars. This improvement is attributed to the filler effect of fine particles and the pozzolanic reactivity of natural pozzolana, which synergistically enhance matrix densification and strength gain. The fine particles optimize the particle packing and reduce porosity, while the pozzolanic reaction with portlandite leads to additional C–S–H formation. This optimization allows some of the mixing water, which would otherwise be trapped in the system, to be freed [63], facilitating better hydration kinetics and workability. Mortar M3, composed of two-thirds marble and one-third pozzolana, demonstrates the highest compressive strength at 7 days (42 MPa), benefiting from the high fineness of marble (BSS = 480 m^2/kg) and the reactivity of pozzolana.

At 28 days, mortars containing only pozzolana (M1) or marble (M4) showed 15% and 12% lower strength, respectively, compared to the limestone-only mix M10. These reductions confirm that despite their fineness, the isolated use of marble or pozzolana does not provide sufficient long-term reactivity or optimal particle packing. Conversely, ternary mortars such as M7 and M9 exhibit superior mechanical performance, reaching 75 MPa and 74 MPa, respectively. This performance is attributed to the combined benefits of high surface area, filler effect, and pozzolanic reaction, leading to refined pore structure and improved bond between the matrix and aggregates. The presence of ultra-fine particles enhances both early and later hydration products, optimizing the microstructure and improving the overall compressive strength.

3.3. Ultrasonic Pulse Velocity

The results of the ultrasonic pulse velocity (UPV) measurements for the mortars are provided in Figure 4.

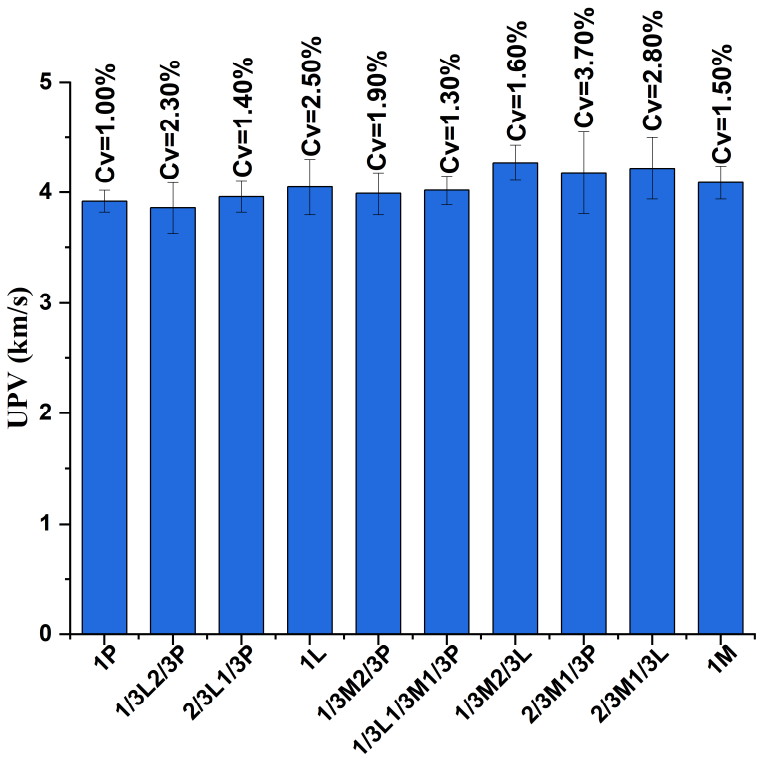

Figure 4. Ultrasonic pulse velocity of mortars.

The results showed a variation in UPV ranging between 3.86 and 4.27 km/s. Mortars primarily including limestone or marble (M7, M8, and M9) exhibited the highest UPV. In contrast, mortars containing pozzolana (M2 and M6) demonstrated lower UPV. This reduction can be attributed to the partial replacement of cement with pozzolana, which not only decreases the amount of hydration products but also increases porosity due to the delayed pozzolanic reaction. Unlike limestone and marble powders, which act as inert fillers and primarily enhance particle packing, pozzolana exhibits latent hydraulic properties. However, its lower short-term reactivity leads to a less compact microstructure at early ages, thereby reducing UPV [64].

3.4. Water Absorption by Immersion

Figure 5 displays the water absorption results for the studied mortars. It is noted that the water absorption of the mortars is closely related to the pore structure and size formed after the mortar has hardened [65,66].

Mortars containing only marble (M5) or pozzolana (M1) exhibit slightly higher water absorption compared to the mortar containing only limestone (M10), with increases of 2% and 3%, respectively. This is attributed to the fine texture and homogeneous distribution of limestone powder within the cement matrix, which reduces voids in this mortar. Mortars with ternary mixes primarily composed of limestone combined with marble or pozzolana (M7 and M9) show lower water absorption compared to mortars with a single powder fraction. The combination of these two fractions creates a new blend with a range of particle sizes that enhances the granular packing of the mortar. Mortars predominantly containing pozzolana in combination with limestone or marble (M2 and M6) exhibit higher water absorption compared to those primarily containing limestone (M7 and M9) or marble (M3). This difference is attributed to increased porosity due to a reduction in hydration products. Mortar M7 has the lowest water absorption at 5.36%, while the highest absorption was observed for mortar M2 at 6.01%.

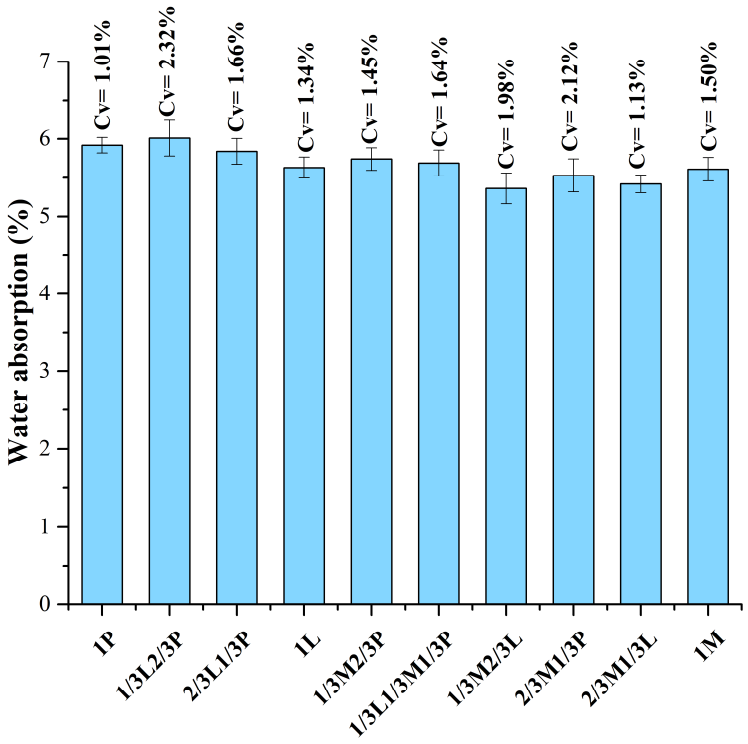

Figure 5. Water Absorption of mortar.

3.5. Capillary Absorption of Mortars

Figure 6 illustrates the capillary curve, with the height of water penetration through capillary pores as a function of the square root of time. Regardless of the type and quantity of additive, the mortars exhibit a similar pattern. The figure reveals two distinct phases. The first phase is an initial rapid increase in absorption depth over the first 24 h, during which approximately 80% of the pores become saturated. This is followed by a more gradual increase in absorption depth.

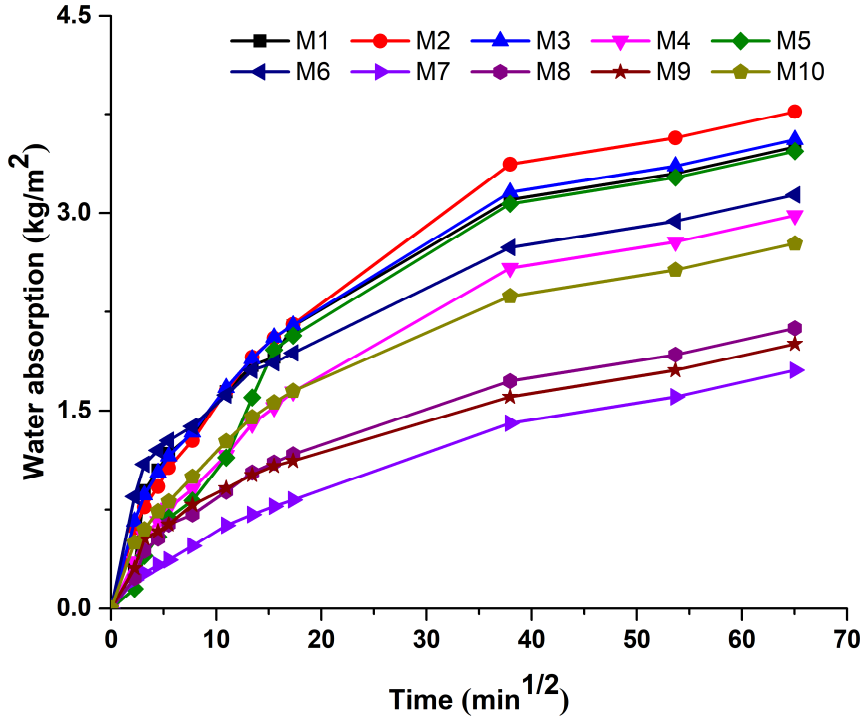

Figure 6. Capillary absorption curve of mortars.

The capillary absorption coefficient for the studied mortars is shown in Figure 7.

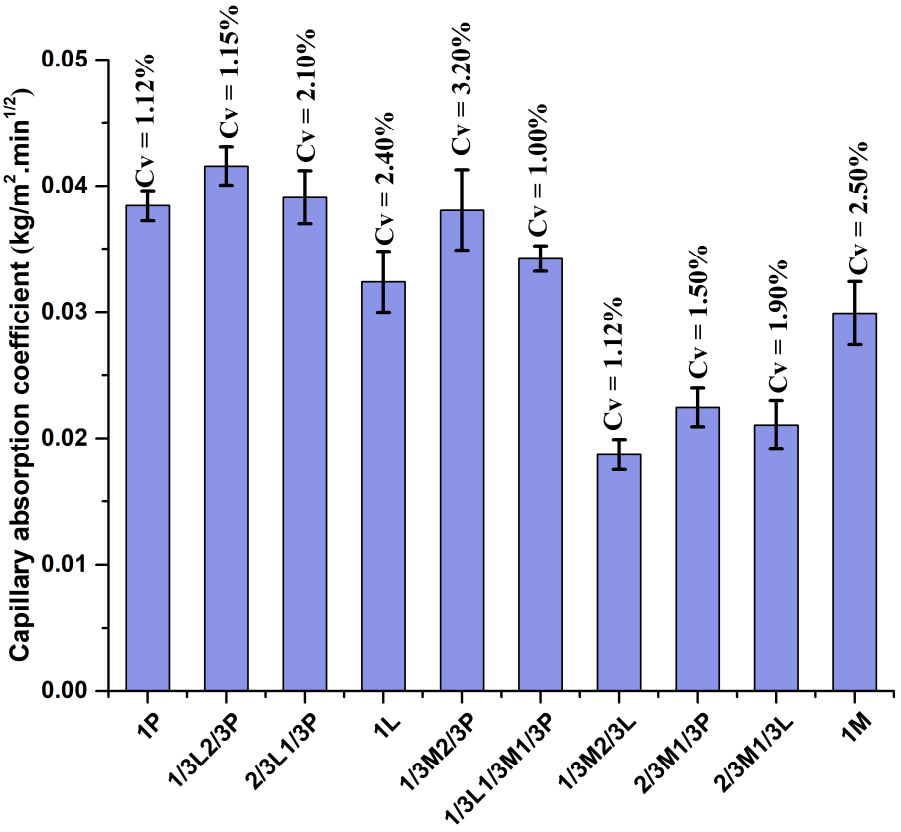

Figure 7. Capillary absorption coefficient of mortars.

The results indicate that mortar M7 has the lowest capillary absorption coefficient due to its high specific surface area of the fillers used, which helps filling voids and results in a denser structure. In contrast, mortar M2 exhibits the highest capillary absorption coefficient. High capillarity values are generally associated with lower compressive strength, which aligns with findings in the literature [67,68]. Mortars with ternary mixes (M3, M5, M6, M7, M8, and M9) show lower capillary absorption coefficient compared to binary mixes (M1, M4, and M10). This can be attributed to the better dispersion and varied particle size distribution of the ternary mixes, covering a broad range of particle sizes. Such heterogeneous distribution effectively fills the pores in the cement matrix, reducing overall porosity and enhancing the mortar's compactness [22].

3.6. Statistical Analysis

The analysis of variance (ANOVA) assesses the contribution of different factors to the observed responses (see Table 3). All models used in this study exhibit relatively acceptable correlation coefficients: 0.91 for slump flow, 0.94 for compressive strength, 0.89 for UPV, 0.96 for water absorption by immersion, and 0.83 for capillary absorption.

Table 3. Summary of the statistical analysis.

	Flow	CS 28	UPV	W	CA
R^2	0.911	0.942	0.896	0.967	0.832
Adjusted R^2	0.799	0.868	0.767	0.925	0.623
Root-mean-square error (RMSE)	0.445	2.669	0.065	0.057	0.005
Mean response	29.64	66.103	4.056	5.675	0.032
Observations (or weighted sums)	10.00	10.00	10.00	10.00	10.00

The ANOVA for each modeled response is presented in Table 4. From this analysis, it can be concluded that the established models are accurate in predicting the combined effects of pozzolana, marble, and limestone powders on the mechanical and physical behavior of self-compacting mortars. For degrees of freedom ddl1 = 5 and ddl2 = 4, with a 95% confidence interval, the critical Fisher value is 6.26. The calculated of ratio between model variance and residual variance (F-values) for slump flow, compressive strength, UPV and absorption by immersion are 8.14, 12.88, 6.89 and 23.20, respectively. Additionally, with an 85% confidence interval, the critical Fisher value is 3.01, and the calculated F-value for immersion absorption is 3.97. These results indicate that the calculated F-values exceed the critical values, thereby confirming the validity of the models. The analysis underscores the robustness of the statistical models in accurately predicting the influence of the different powders on the mortar's properties. The high F-values, particularly for compressive strength and capillary absorption, demonstrate the significant impact of these factors on the mortar's behavior, ensuring that the predictions align well with the experimental data.

Table 4. ANOVA analysis for the studied responses.

	Source	df	Sum of Squares	Mean Square	F Ratio
Flow test	Model	5	8.070	1.614	8.14
	Error	4	0.794	0.198	Prop. > F
	Uncorrected Total	9	8.864		0.032
CS 28	Model	5	458.80	91.760	12.88
	Error	4	28.49	7.123	Prop. > F
	Uncorrected Total	9	487.29		0.014
UPV	Model	5	0.144	0.028	6.89
	Error	4	0.016	0.004	Prop. > F
	Uncorrected Total	9	0.161		0.00424
W	Model	5	0.382	0.076	23.20
	Error	4	0.013	0.003	Prop. > F
	Uncorrected Total	9	0.395		0.01047
CA	Model	5	0.001	0.0000103	3.97
	Error	4	0.000	0.0000026	
	Uncorrected Total	9	0.001		

Full cubic model equations were developed to predict the slump flow, compressive strength, immersion absorption, and capillary absorption of mortars with a 20% partial replacement of cement by pozzolana, marble, and limestone powders. These equations (from Equations (16)–(20)) account for the complex interactions between the different components, enabling accurate modeling of the physical and mechanical properties of the mortars within the studied range. The use of full cubic model captures not only linear effects but also quadratic and interaction effects between the variables, providing a more precise prediction of the mortars' performance.

This approach allows for a comprehensive understanding of how each component influences the overall behavior of the mortar, considering the non-linear relationships that are often present in such systems. The ability to model these interactions is crucial for optimizing mortar formulations, ensuring that the predicted properties align closely with experimental results, and facilitating the development of mortars with desired characteristics.

$$Flow\ (\mathrm{cm}) = 27.89 \times PZ + 29.32 \times L + 29.38 \times M + P \times (0.83 \times L) + P \times (7.90 \times M) + L \times (5.14 \times M) \quad (16)$$

$$CS\ 28(\mathrm{MPa}) = 57.92 \times P + 69.81 \times L + 70.373 \times M + P \times (-32.92 \times L) + P \times (10.86 \times M) + L \times (21.05 \times MR) \quad (17)$$

$$UPV\ (\mathrm{km/s}) = 3.90 \times P + 4.08 \times L + 4.11 \times M + P \times (-0.43 \times L) + P \times (0.28 \times M) + L \times (0.61 \times M) \quad (18)$$

$$W(\text{cm}) = 5.94 \times P + 5.60 \times L + 5.60 \times M + P \times (0.76 \times L) + P \times (-0.53 \times M) + L \times (-0.88 \times M) \quad (19)$$

$$CA(\text{cm}) = 0.039 \times P + 0.031 \times L + 0.027 \times M + P \times (0.026 \times L) + P \times (-0.011 \times M) + L \times (-0.039 \times M) \quad (20)$$

To determine which factors and interactions significantly influence the studied properties and guide the optimization of material formulations, an ANOVA analysis was performed and is presented in Table 5.

Table 5. ANOVA summary for the full cubic model.

	Flow		**CS 28**		**UPV**		**W**		**CA**	
Model	**F Ratio**	***p*-Value**	**F Ratio**	***p*-Value**	**F Ratio**	***p*-Value**	**F Ratio**	***p*-Value**	**F Ratio**	***p*-Value**
A-P	4429.2	<0.0001 *	531.9	<0.0001 *	4111.15	<0.0001 *	12,077.4	<0.0001 *	68.7639	0.0012 *
B-L	4894.44	<0.0001 *	772.47	<0.0001 *	4486.49	<0.0001 *	10,750.2	<0.0001 *	42.5829	0.0028 *
C-M	4913.53	<0.0001 *	793.01	<0.0001 *	4559.09	<0.0001 *	10,728.2	<0.0001 *	33.9714	0.0043 *
(A) · (B)	0.2028	0.6758	8.76	0.0415 *	2.55	0.185	10.0607	0.0338 *	1.5592	0.2799
(A) · (C)	18.15	0.013 *	0.95	0.3838	1.1	0.353	4.9776	0.0895	0.2907	0.6184
(B) · (C)	7.68	0.0503	3.58	0.1312	5.13	0.086	13.5614	0.0212 *	3.4038	0.1388

*: (Prob. > F) very lower than 5%.

Table 5 summarizes the ANOVA results, highlighting the most statistically significant effects. Key indicators include probability of observing the effect by chance (*p*-values), which indicate significance (threshold < 0.05), and F-ratios, which reflect the relative contribution of each factor to response variability. The main factors P, L, and M exhibit highly significant effects on all response variables, as evidenced by consistently low *p*-values. In contrast, most interaction terms show limited influence, with exceptions observed for specific properties: interaction (A)(C) significantly affects flow, (A)(B) impacts CS28, and both (A)(B) and (B)(C) influence absorption. Overall, the ANOVA confirms the robustness and validity of the developed models, and identifies the key parameters driving the behavior of the tested mortars, thereby reinforcing the reliability of the experimental findings and supporting their application in predictive mix design optimization.

Figure 8 illustrates the relationship between the predicted and measured values of the studied responses, with 95% confidence intervals (solid red line) for slump flow, compressive strength, and capillary absorption, as well as an 85% confidence interval for adsorption by immersion. The results demonstrate that the models developed in this study align closely with the data from the literature on the use of powders in mixtures, obtained through the mix design method. The high correlation coefficients (R^2 ranging from 0.87 to 0.99) indicate a strong agreement between the predicted outcomes and the experimental data.

This close correspondence highlights the reliability of the models in capturing the essential behaviors of mortars with partial cement replacement by pozzolana, marble, and limestone powders. The inclusion of confidence intervals further reinforces the robustness of the predictions, ensuring that the modeled responses accurately reflect the variability observed in experimental settings. The strong correlation also underscores the models' utility in predicting mortar properties across different compositions within the studied range.

Figure 9 presents the iso-response curves derived from second-order polynomial equations for four key properties of self-compacting mortars: slump flow, compressive strength, absorption by immersion, and capillary absorption. These iso-response curves aid in predicting mortar performance and help identify optimal compositions for further study.

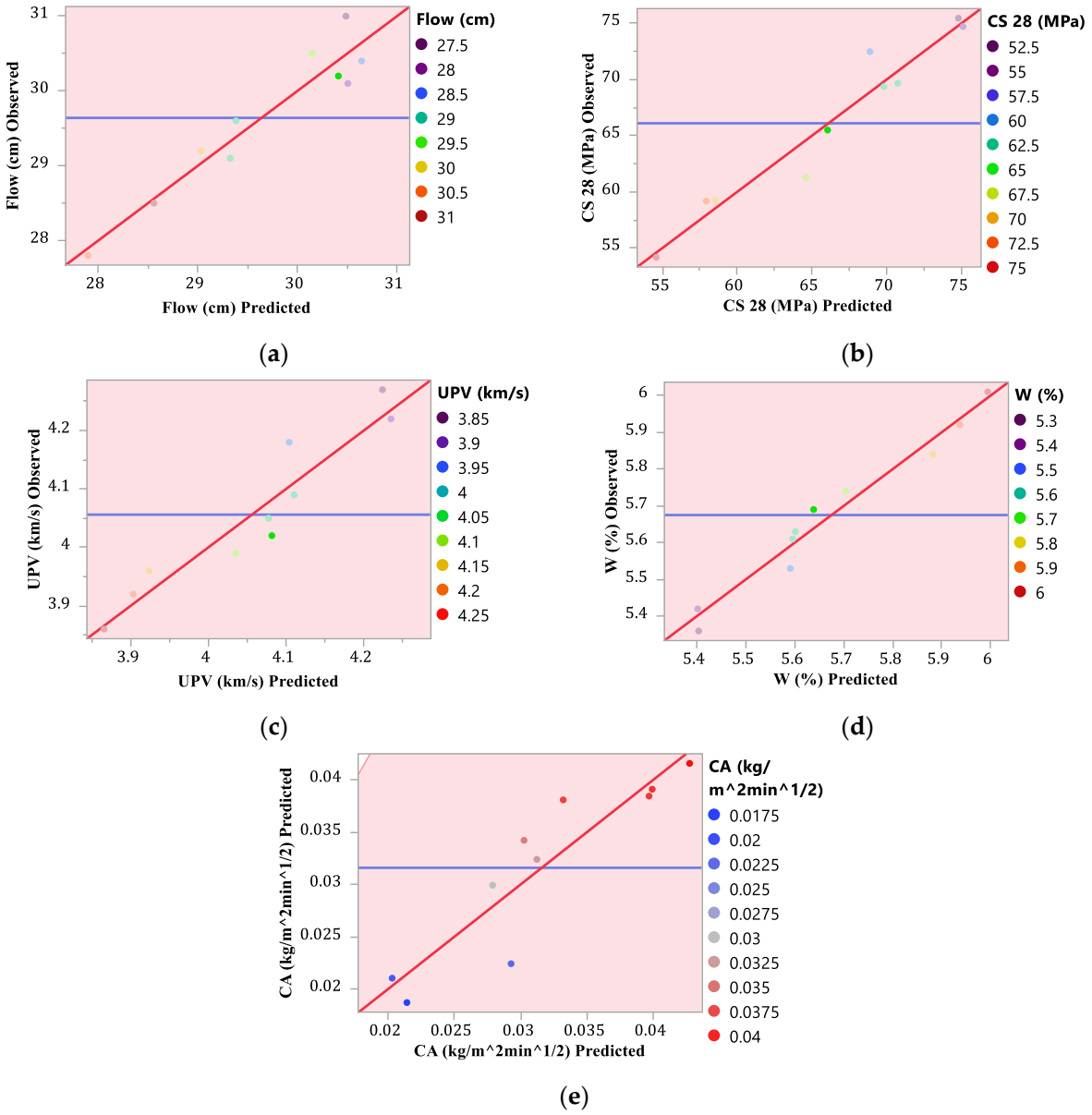

Figure 8. Actual vs. predicted: (**a**) flow; (**b**) compressive strength at 28 days; (**c**) UPV; (**d**) absorption by immersion; (**e**) capillary absorption.

Figure 10 illustrates the influence of the various additives on the studied responses. The incorporation of natural pozzolana into self-compacting cement mortars leads to a reduction in fluidity, primarily due to its high-water absorption capacity, which increases the water demand of the mix and, consequently, reduces its flowability. Furthermore, the addition of pozzolana results in a decrease in mechanical strength, likely due to a dilution effect that reduces the proportion of active clinker in the mix. Simultaneously, there is an increase in both capillary and by immersion absorption, which can be attributed to the increased porosity of the mortar caused by the pozzolana. In contrast, the inclusion of marble and limestone powders enhances slump flow and mechanical strength up to optimal values of 0.49 and 0.51, respectively. This beneficial effect is due to the fineness of these powders, filling the voids between cement particles and increasing the density of the mortar, thereby improving its mechanical properties. However, beyond these optimal values, an excess of powder can lead to an overload of fines, which increases the viscosity of the mortar, negatively affecting fluidity and reducing compaction, thus diminishing mechanical strength. Additionally, the effect of marble powder on immersion and capillary

absorption is inversely proportional to its content in the mortar. A low proportion of marble powder can reduce porosity, while an excessive amount can result in the formation of interconnected pores, thereby increasing water absorption.

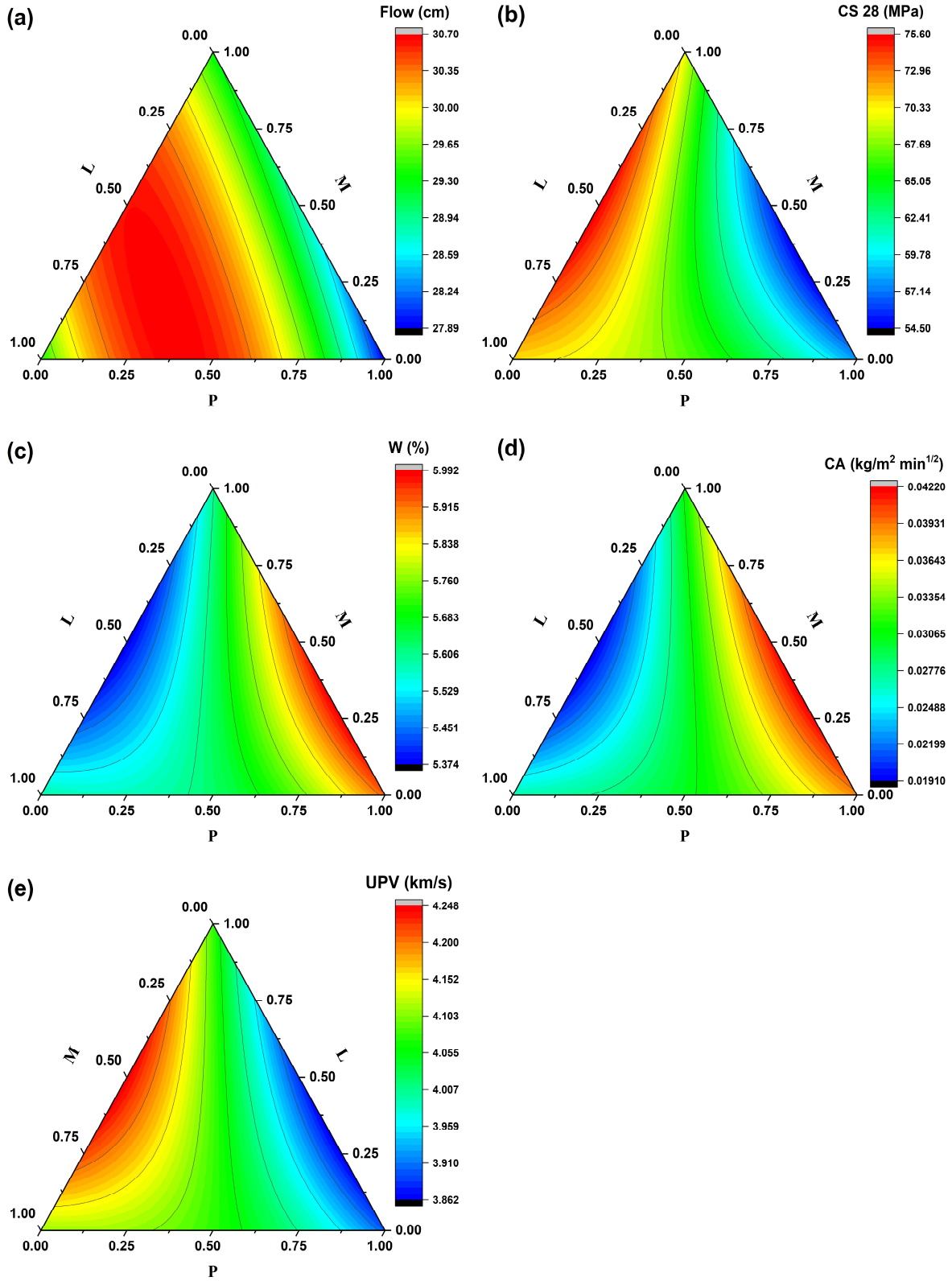

Figure 9. Iso-response curves for: (**a**) slump flow; (**b**) compressive strength; (**c**) water absorption by immersion; (**d**) water absorption by capillarity and (**e**) UPV.

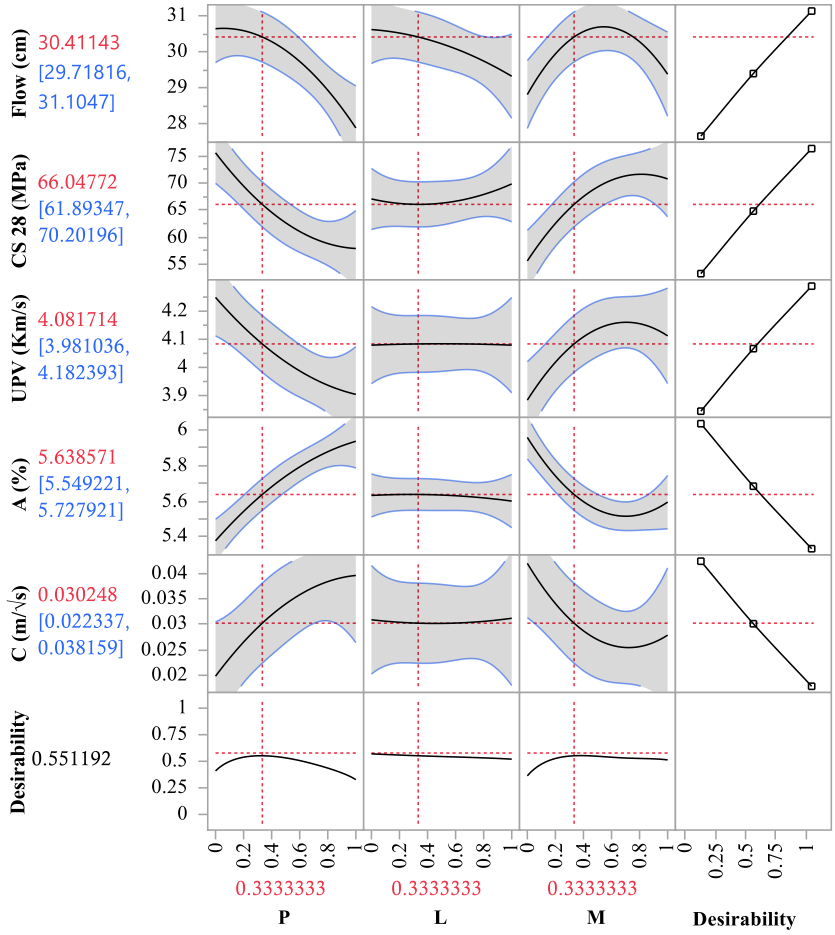

Figure 10. Main effect on mortars of the studied parameters.

To optimize and define the adequate mortar formulations, the desirability of each property was adjusted according to the following objectives: maximizing the mortar's slump flow to achieve greater fluidity, maximizing compressive strength to attain high values, and minimizing both absorption by immersion and capillary to create mortars more resistant to water penetration. These adjustments allow for the formulation of mortars that meet specific requirements in terms of workability, durability, and mechanical performance. The effectiveness of the optimization models is summarized in Table 6, demonstrating their capability in achieving desired mortar characteristics. This comprehensive approach ensures that the selected mortar compositions offer an optimal balance between ease of application and long-term durability, making them suitable for a wide range of construction applications. The use of second-order polynomial equations in this context enables precise fine-tuning of mortar components to meet specific performance goals.

Table 6. The four most efficient optimized mortar formulations based on overall desirability scores.

	OM1	OM2	OM3	OM4
(A) P	0.004	0.004	0.023	0.100
(B) M	0.535	0.385	0.264	0.254
(C) L	0.461	0.611	0.713	0.646
F (min)	30.631	30.586	30.436	30.596
CS 28 (MPa)	75.332	75.247	74.139	72.537
UPV (km/s)	4.242	4.240	4.214	4.189
W (%)	5.384	5.392	5.435	5.472
AC ($mm/s^{1/2}$)	0.020	0.020	0.022	0.023
Desirability	0.894	0.888	0.833	0.793

4. Life Cycle Assessment of Studied Self-Compacting Mortars

The cement industry is characterized by high energy consumption, extensive use of natural resources, and substantial greenhouse gas (GHG) emissions. It is among the largest contributors to global GHG emissions, accounting for 1.6×10^9 tons of CO_2 in 2022, representing approximately 8% of total global CO_2 emissions [69]. In Algeria, the production of one ton of cement requires 5.716 GJ of energy and generates 882 kg of CO_2 equivalent [70]. As a key component of mortar, cement acts as a binder that ensures aggregate cohesion and contributes to the material's mechanical performance. Through hydration, it progressively develops the strength necessary for structural stability. A standard cubic meter of mortar contains approximately 705 kg of cement, accounting for nearly 30% of its total mass. The production of this cement is associated with significant carbon emissions, primarily due to the calcination of limestone ($CaCO_3 \rightarrow CaO + CO_2$) and the combustion of fossil fuels in clinker manufacturing.

Given these environmental concerns, this study assesses the ecological footprint of the investigated mortars through a Life Cycle Assessment (LCA). The primary objective is to quantify the carbon footprint of each mixture and enable a comparative analysis. Two key environmental indicators are considered: GHG emissions and the depletion of non-renewable energy resources. Additionally, this study examines the effects of material processing, transportation, and energy consumption on the overall sustainability of self-compacting mortars. To ensure a robust comparative assessment, ten mortar production scenarios were modeled using the specialized LCA software Activity Browser (version 2.11.1), which integrates the EcoInvent database (version 3.10) comprising over 23,500 processes for environmental modeling. The selected impact assessment method, CML-IA baseline, quantifies GHG emissions in CO_2-equivalents and evaluates the depletion of non-renewable energy resources.

4.1. Study Assumptions

The proposed scenarios were adjusted to best represent real industrial conditions in Algeria. Additional assumptions were made to enhance the accuracy of the models while maintaining analytical rigor. The key assumptions are as follows:

- A uniform transport distance of 150 km was adopted in the modeling due to the lack of precise extraction site data. This assumption enables the integration of transportation impacts into the environmental balance while avoiding bias in favor of or against any specific material based on geographic proximity. It represents a plausible and regionally representative estimate, ensuring fair comparability among raw materials.
- Unlike pozzolana, which is considered a natural resource, limestone and marble were treated as recycled construction waste in the modeling. This distinction is critical, as recycled materials generally have a lower environmental impact due to the avoided extraction phase.
- Due to differences in hardness, marble requires more electrical energy for grinding than limestone (0.06 kWh vs. 0.04 kWh per unit weight, respectively). This factor significantly influences the overall energy balance of the different mortar formulations.
- Mortar mixing and preparation were assumed to be manual, requiring no additional electrical energy. This assumption aligns with small-scale production scenarios but may differ in large industrial applications.

4.2. Impact of Greenhouse Gas Emissions and Non-Renewable Energy Resources on the Studied Mortars

Mortar consists mainly of sand and cement, with the latter significantly influencing its environmental impact. According to the study's findings (see Figure 11), producing one

cubic meter (2290.575 kg) of mortar generates 615.105 kg of CO_2 equivalent and consumes 3157.867 MJ of non-renewable energy (primarily natural gas and petroleum). Cement production accounts for over 83.31% of GHG emissions and 90% of total energy demand, reinforcing the importance of optimizing cement use in mortar formulations.

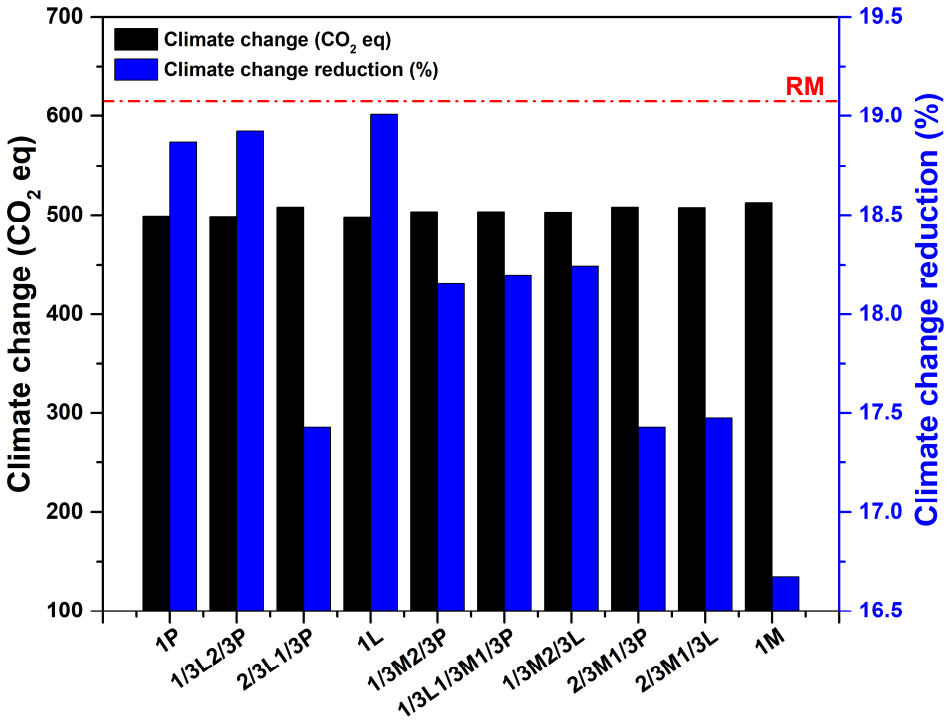

Figure 11. Carbon footprint effects on the studied self-compacting mortars.

Replacing cement in mortar formulations led to positive environmental outcomes, reducing GHG emissions by up to 19% (M4) and lowering energy consumption by 17.21% (M1) (Figure 12). However, these results consider only environmental aspects and do not provide a comprehensive analysis of the modified mortars' technical performance. Future studies should integrate mechanical and durability assessments to ensure that the proposed substitutions maintain or enhance structural properties.

In Algeria, the energy mix is overwhelmingly dominated by fossil fuels, accounting for 99% of total supply, with natural gas alone representing 64.9%, while renewable sources contribute only about 0.4%. The local abundance of natural gas, combined with its low and stable cost, currently makes its substitution with alternative energy sources technically and economically challenging, despite being desirable in the long term. Nevertheless, the gradual integration of alternative energy sources into cement production offers a promising pathway to mitigate the environmental footprint of this highly CO_2-intensive sector. Utilizing low-carbon or renewable energy such as biomass, refuse-derived fuels (RDF), green hydrogen, or solar thermal energy can significantly reduce greenhouse gas emissions, enhance energy security, and support waste valorization within a circular economy framework. A thorough assessment of the environmental and techno-economic relevance of such alternatives, specifically within the Algerian context, represents a strategic research perspective and will be the subject of future publications.

To comprehensively evaluate the technical and environmental performance of the studied mortars, compressive strength and greenhouse gas (GHG) emissions were analyzed together and presented in Figure 13. Marble-based mixtures (M8, M9, and M10) exhibited the lowest GHG reduction rates, with values of 17.43%, 17.47%, and 16.67%, respectively. Despite their lower environmental benefits, these formulations demonstrated notable

improvements in compressive strength, increasing by +11%, +10%, and +2%, respectively. This trade-off arises from the higher energy demand associated with marble processing, which is counterbalanced by its densification effect within the mortar matrix, thereby enhancing mechanical performance.

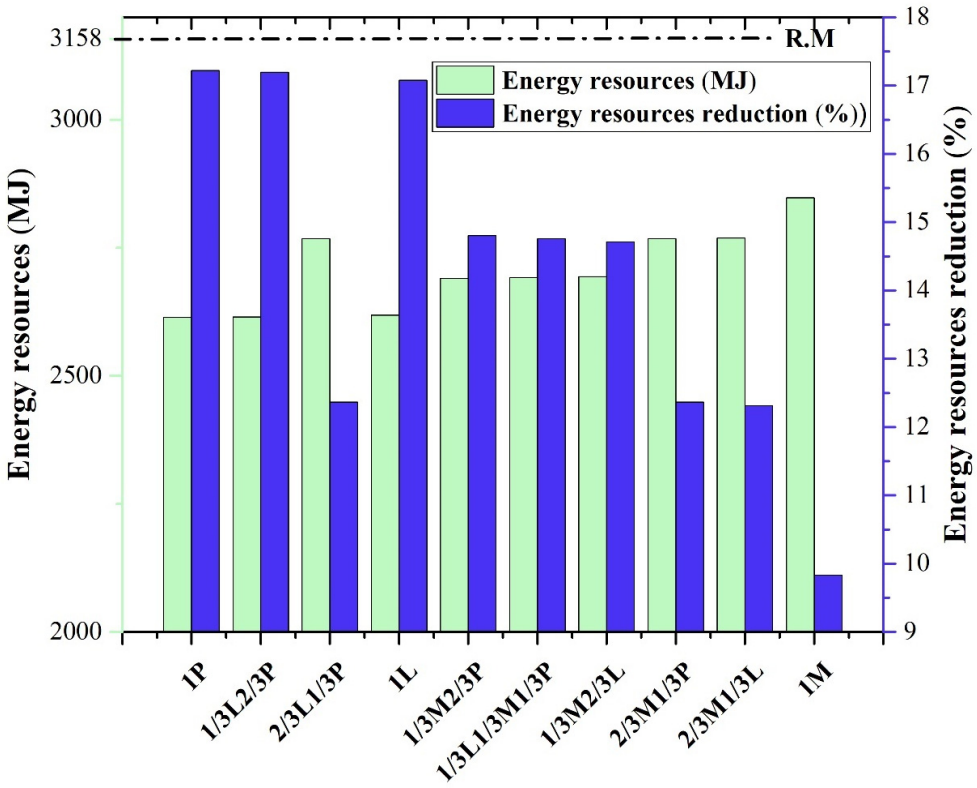

Figure 12. Energy resource impact on the studied self-compacting mortars.

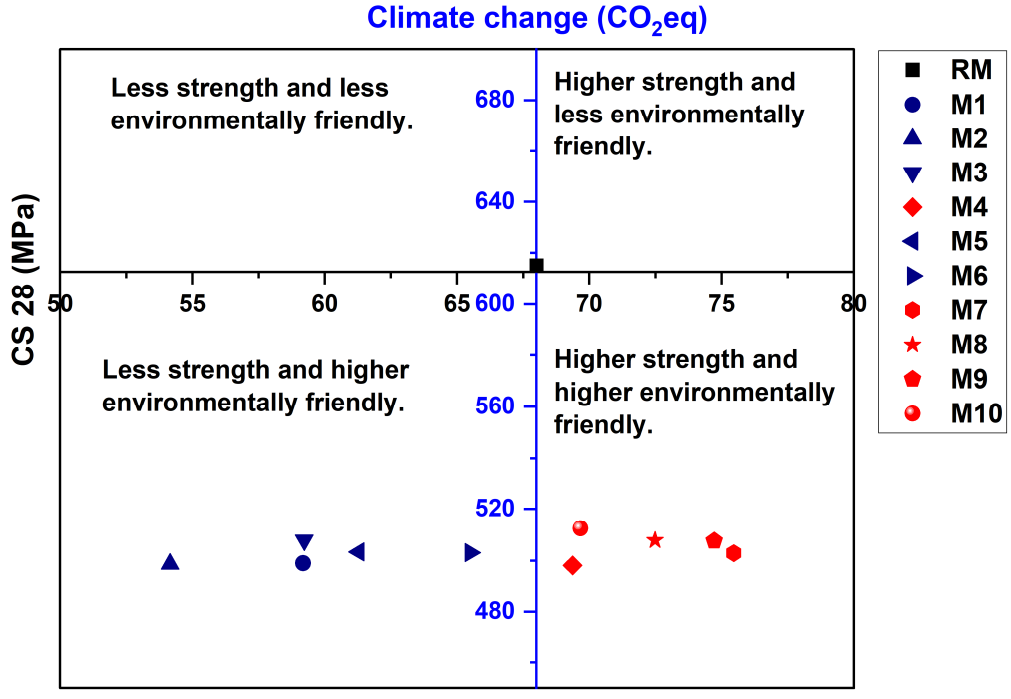

Figure 13. Techno-environmental efficiency of self-compacting mortars.

Limestone-based mixtures (M6 and M7) achieved moderate GHG reductions of 18.20% and 18.24%, corresponding compressive strength variations of −4% and +7%, respectively. Among all formulations, M4 emerged as the most advantageous scenario, attaining the highest GHG reduction (19.01%) while maintaining a +2% increase in compressive strength. The superior performance of limestone-based mortars is attributed to their lower grinding energy requirements than marble and their ability to enhance particle packing density, thereby improving mechanical properties.

GHG emissions are strongly correlated with the consumption of non-renewable resources, primarily due to hydrocarbon combustion. The trends in non-renewable energy consumption closely align with those of GHG emissions, with pozzolana-based mixtures (M1 and M2) achieving the highest reductions (17.22% and 17.20%) at the cost of decreased mechanical performance (−13% and −20%). Limestone-based formulations (M4, M6, and M7) followed, with reductions of 17.08%, 14.76%, and 14.71%, respectively, and strength variations of +2%, −4%, and +7%. Conversely, marble-based mixtures (M8, M9, and M10) exhibited the lowest reductions (12.36%, 12.32%, and 9.83%) while achieving the highest strength gains (+11%, +10%, and +2%). Overall, M4, M7, M8, M9, and M10 are identified as both high-performing and environmentally beneficial compared to the reference mortar (Figure 13), as they combine improved compressive strength with lower GHG emissions. In contrast, while demonstrating significant environmental impact reductions, M1, M2, M3, M5, and M6 exhibit lower mechanical performance (Figure 13), positioning them as more sustainable yet mechanically less efficient alternatives.

5. Discussion

Analyzing the results in this study, the authors compare their findings within the other across the literature. In case of the slump flow, investigated mortars containing marble powder exhibited higher flows compared to those containing limestone and pozzolana powders. This can be attributed to the morphology and external texture of marble, which is typically angular and relatively rounded with a smooth surface, enhancing its affinity and dispersion as also presented in [71]. Conversely, limestone powder has an irregular shape with a rough surface texture, which can increase the demand for water or water-reducing admixtures to overcome internal friction during flow [72]. The natural pozzolana absorbs a portion of the water needed for hydration, reacting with portlandite to form C-S-H gel, leading to a reduction in mortar flow [73]. Similar results, to ours that pozzolana decreases consistency of cement pastes due to high water consumption during hydration were found by Ezziane et al. [74]. In addition, Belaidi et al. [35] investigated binary effects with substitution ratios up to 10% for both marble and pozzolana powders, concluding that mortars containing marble powder exhibit superior rheological properties compared to those containing pozzolana, likely due to higher water demand. These findings are consistent with the results obtained in the present study as well.

Analyzing the mechanical properties, Turkel et al. [75] observed that substituting cement with a small amount of limestone powder (5 to 15%) combined with other additives had a predominantly positive effect on mechanical properties. The increase in compressive strength can be explained by the filling effect of finely ground limestone powder [76]. Furthermore, combining two powders of different fineness results in a granular structure that can fill voids of various sizes. Guneyisi et al. [77] found that ternary binder mortars helped mitigate the drawbacks of binary mortars with binder composed of cement and fly ash. Thus, the compressive strengths of mortars with 10% of fly ash and 10% of metakaolin were higher than those of the reference mortar. Furthermore, Ghrici et al. [48] also demonstrated that 10% of limestone combined with a small quantity of additive with

pozzolanic characteristics positively contributes to early-age compressive strength. These all findings are consistent with the results obtained in the present study.

Furthermore, the primary effect of adding limestone is likely a filling effect [78], which improves the microstructure within the paste matrix and the transition zone, leading to an increase in UPV [79]. Moreover, pozzolana is known for its pozzolanic properties, while limestone and marble are generally considered relatively inert fillers [80]. Specifically, $CaCO_3$, the main component of these powders, is reported to accelerate the hydration of C3S, resulting in enhanced early-age compressive strength [81,82].

It is important to note that the physical and chemical characteristics of raw materials such as limestone, marble, and pozzolana can vary significantly depending on their geological origin and processing methods. Differences in mineral composition, particle size distribution, and surface morphology may influence reactivity, water demand, and workability, which in turn affect hydration kinetics and strength development. This variability can compromise the reproducibility and generalizability of results, particularly when comparing across studies or scaling up to industrial applications.

Additionally, factors such as mixing procedures, ambient temperature, and especially curing conditions play a decisive role in the performance of cement-based composites. In this study, all specimens were cured in a controlled environment at 20 $\pm$ 2 °C and a relative humidity above 95% to ensure optimal hydration. Such conditions are critical for the formation of calcium silicate hydrate (C–S–H) gel and for enabling the pozzolanic reaction between pozzolana and portlandite. Inadequate or inconsistent curing could result in incomplete hydration or delayed strength gain, potentially obscuring the true material behavior. Therefore, standardization and rigorous control of both raw material properties and curing protocols are essential to ensure the accuracy, comparability, and applicability of experimental results [83,84].

Building on the above statements, which strengthen our reasoning and support the validity of the obtained results, we not only provide the predictive equations for specific properties but also analyze potential predictions or correlations between the investigated properties.

In case of the 28 days compressive strength, we observed very high correlation between this property and experimentally obtained UPV, water absorption by immersion and capillary absorption, that is visualized in Figure 14.

It can be observed that as the ultrasonic pulse velocity increases, the compressive strength also increases, regardless of the mortar mixture. In contrast, the compressive strength of hardened mortars decreases with higher water absorption by immersion and capillary action. This aspect is beneficial from a design perspective, as any type of additive, whether pozzolanic, marble powder, or limestone powder, maintains a linear correlation between these properties and compressive strength. What is also worth mentioning is the fact that capillary absorption and water absorption by immersion are also linearly correlated, which is depicted in Figure 15.

Although the predictive equations developed in this study demonstrate strong statistical correlations within the experimental dataset, they have not yet been validated against independent datasets. Therefore, future research should focus on testing these models using external or real-scale data to assess their robustness and generalizability across different material sources and curing conditions.

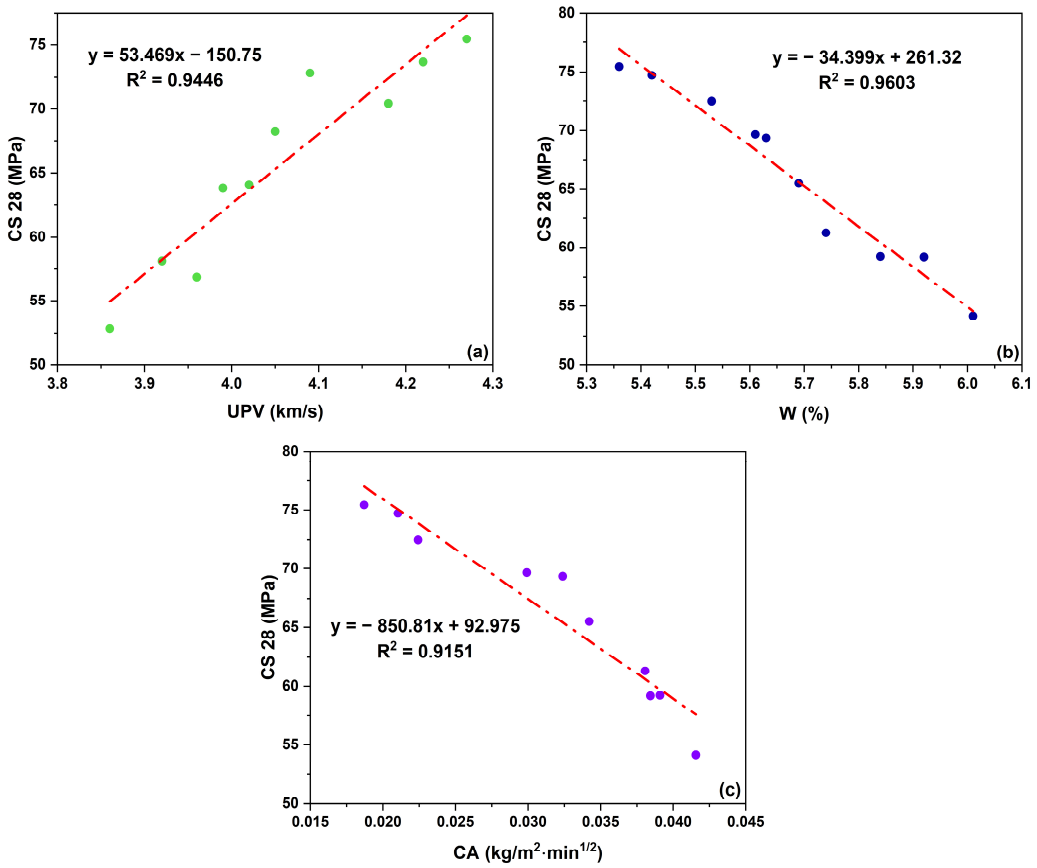

Figure 14. Correlation between the compressive strength and (**a**) UPV, (**b**) water absorption by immersion and (**c**) capillary absorption.

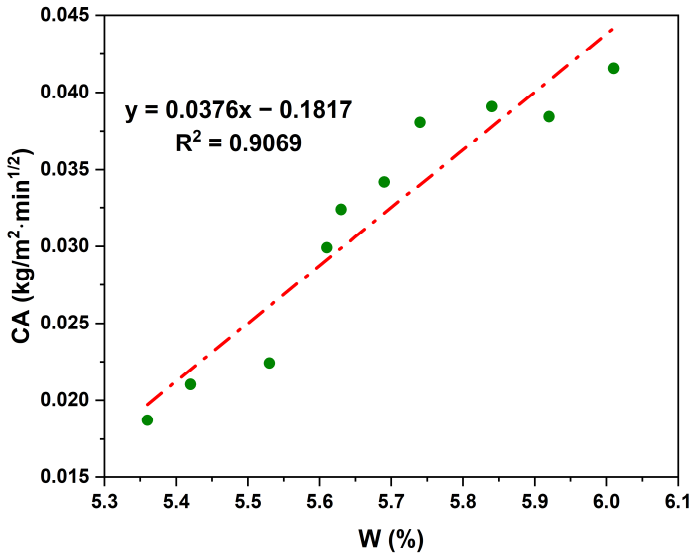

Figure 15. Correlation between the water absorption by immersion and capillary absorption.

6. Conclusions

The present study highlights the benefits of optimizing self-compacting mortars through partial substitution of cement with pozzolana, limestone, and marble powders, namely using ternary additions. The mix design was conducted using the mixture design method to systematically analyze the interactions between these mineral additions and optimize their combined effect. The results obtained show that the following:

- Mortars containing marble powder exhibited superior flowability, with a spread value reaching up to 32 cm, outperforming other mixtures by up to 9%.
- The results highlight that Blaine specific surface alone does not govern compressive strength. Despite its high fineness (480 m^2/kg), marble led to 12% lower strength at 28 days compared to limestone (422 m^2/kg). In contrast, ternary blends combining high BSS and pozzolanic reactivity (e.g., M7, M9) achieved the highest strengths (up to 75 MPa), confirming that optimized synergy between surface area and reactivity is key to mechanical performance.
- The UPV values ranged from 3.86 to 4.27 km/s, with the highest values observed in mortars containing limestone or marble due to their filler effect, which improves the microstructure. In contrast, pozzolana substitution led to lower UPV due to its delayed pozzolanic reaction and increased porosity. A strong correlation (R^2 = 0.94) was found between compressive strength and UPV, confirming UPV as a reliable indicator of the mechanical performance of self-compacting mortars.
- Water absorption tests indicated that mortars containing powders of marble (M5) or natural pozzolana (M1) had slightly higher water absorption by immersion than those with only limestone powder (M10), with increases of 2% and 3%, respectively.
- The capillary analysis revealed that marble powder contributed to the lowest capillary coefficient, likely due to its high specific surface area.
- Statistical analysis, including R^2 and ANOVA, validated the effectiveness of the models in predicting flowability, 28-day compressive strength, water absorption, and capillarity.
- The optimization process successfully identified the most effective mortar formulations, balancing these properties to meet specific performance criteria.
- The partial replacement of cement in mortar formulations led to a reduction in GHG emissions by up to 19.01% (M4) and a decrease in non-renewable energy consumption by up to 17.22% (M1). Pozzolana-based mixtures demonstrated the most significant environmental benefits, with emission reductions of 18.87% (M1) and 18.92% (M2), while marble-based mixtures exhibited the lowest reductions, reaching only 9.83% (M10).
- Limestone substitution proved to be an effective alternative, achieving emission reductions of up to 18.24% (M7) and energy savings of 14.76% (M6). However, the environmental benefits of cement reduction must be assessed alongside mechanical and durability performance to ensure that these optimized formulations maintain or enhance structural integrity.
- This study provided a comprehensive evaluation of the mechanical, environmental, and durability performance of various blended mortar formulations incorporating pozzolana, limestone, and marble powders. The results highlight a performance trade-off between compressive strength and environmental impact, largely governed by the nature and proportion of the supplementary materials. Marble-based mortars (M8–M10) exhibited the highest strength improvements but delivered modest reductions in GHG emissions, due to their higher energy footprint. In contrast, pozzolana-based mixes (M1, M2) achieved the greatest environmental gains, albeit at the cost of lower mechanical performance. Limestone-based mixtures, particularly M4, demonstrated the most balanced profile, combining a notable GHG reduction (19.01%) with a modest strength gain (+2%), confirming its suitability for sustainable and high-performance applications. Overall, the findings underscore the importance of holistic mix design strategies that integrate technical properties, durability criteria, and life cycle impacts to guide the development of environmentally optimized mortars for the construction sector.

An in-depth analysis of the economic and environmental impacts of incorporating these materials into self-compacting mortars would be highly valuable, focusing on aspects such as cost-effectiveness, CO_2 emissions reduction, and resource sustainability. Additionally, a detailed investigation into the microstructural changes induced by these additions is crucial to understand the mechanisms behind the observed improvements in mortar properties. This combined approach will not only enhance the practical application of these materials but also provide insights into their long-term benefits and viability in sustainable construction practices.

For future work, the same dataset will be employed to develop robust mathematical models of the studied parameters using advanced modeling techniques, including machine learning and response surface methodology. Combinatorial optimization will be explored as a powerful strategy for deriving multi-objective solutions—balancing mechanical performance, environmental impact, and cost—with minimal computational effort. To enhance the practical relevance of the findings, future studies will also focus on validating the developed models in real-world construction scenarios, such as pilot-scale applications or site-based mortar performance assessments. This will enable the translation of theoretical predictions into tangible engineering outcomes, thereby strengthening the models' reliability and applicability.

Author Contributions: C.B., L.M., P.F., H.A., S.C. and A.C.; Data curation, A.D., A.M., K.H. and M.B.; Formal analysis, S.C. and A.C.; Funding acquisition, A.D., A.M., L.M. and P.F.; Investigation A.D., A.M., L.M., P.F., H.A., S.C. and A.C.; Methodology, K.H., M.B., C.B., L.M., P.F., S.C. and A.C.; Project administration, K.H., M.B. and C.B.; Resources, A.D., A.M., K.H., M.B., C.B. and H.A.; Software, K.H., M.B., C.B., L.M., P.F., S.C. and A.C.; Supervision, A.D., A.M. and C.B.; Validation, A.D., A.M., K.H. and M.B.; Visualization, A.D., A.M., L.M., P.F., H.A., S.C. and A.C.; Writing—original draft, K.H., M.B., C.B., L.M., P.F., H.A., S.C. and A.C.; Writing—review and editing, A.D., A.M., K.H., M.B., C.B., L.M., P.F., H.A., S.C. and A.C. All authors have read and agreed to the published version of the manuscript.

Funding: This research received no external funding.

Institutional Review Board Statement: Not applicable.

Data Availability Statement: The data presented in this study are available on request from the corresponding author.

Conflicts of Interest: The authors declare no conflicts of interest.

References

1. Shah, I.H.; Miller, S.A.; Jiang, D.; Myers, R.J. Cement substitution with secondary materials can reduce annual global CO_2 emissions by up to 1.3 gigatons. *Nat. Commun.* **2022**, *13*, 5758. [CrossRef] [PubMed]
2. Chaudhury, R.; Sharma, U.; Thapliyal, P.; Singh, L. Low-CO_2 emission strategies to achieve net zero target in cement sector. *J. Clean. Prod.* **2023**, *417*, 137466. [CrossRef]
3. Mora, P.; Sanjuán, M.; Moraño, A.; Fernández-Hernández, M. Cement Sector and Promising Technologies to Reduce CO_2 Footprint Through Circular Economy: Novel Raw Materials and Products. In *Circular Economy on Energy and Natural Resources Industries: New Processes and Applications to Reduce, Reuse and Recycle Materials and Decrease Greenhouse Gases Emissions*; Springer: Cham, Switzerland, 2024; pp. 53–71.
4. Teker Ercan, E.E.; Andreas, L.; Cwirzen, A.; Habermehl-Cwirzen, K. Wood Ash as Sustainable Alternative Raw Material for the Production of Concrete—A Review. *Materials* **2023**, *16*, 2557. [CrossRef]
5. Jittin, V.; Bahurudeen, A. Production of cleaner binders by reusing agricultural by-products: An approach towards zero cement concrete for sustainable future infrastructure. *J. Clean. Prod.* **2024**, *451*, 141990. [CrossRef]
6. Akram, R.; Ibrahim, R.L.; Wang, Z.; Adebayo, T.S.; Irfan, M. Neutralizing the surging emissions amidst natural resource dependence, eco-innovation, and green energy in G7 countries: Insights for global environmental sustainability. *J. Environ. Manag.* **2023**, *344*, 118560. [CrossRef]

7. Ghulam, S.T.; Abushammala, H. Challenges and opportunities in the management of electronic waste and its impact on human health and environment. *Sustainability* **2023**, *15*, 1837. [CrossRef]
8. Aravecchia, N.; Bañuls-Ciscar, J.; Caverzan, A.; Ceccone, G.; Cuenca, E.; Ferrara, L.; Grigoriadis, K.; Negro, P.; Rodriquens, M. On the feasibility of using Polyester (PE) waste particles from metal coating industry as a secondary raw materials in concrete. *Clean. Mater.* **2023**, *9*, 100193. [CrossRef]
9. Anandaraj, S.; Karthik, S.; Elango, K.; Nishiketan, S.; Pandiyarajan, G.; Kumar, P.N.; Palanikumar, R.; Harihanandh, M. An experimental study on Fly Ash (FA) and marble powder in the properties of Self-Compacting Concrete (SCC). *Mater. Today Proc.* **2022**, *52*, 1771–1774. [CrossRef]
10. Nasr, M.S.; Salman, A.J.; Ghayyib, R.J.; Shubbar, A.; Al-Mamoori, S.; Al-khafaji, Z.; Hashim, T.M.; Hasan, Z.A.; Sadique, M. Effect of clay brick waste powder on the fresh and hardened properties of self-compacting concrete: State-of-the-art and life cycle assessment. *Energies* **2023**, *16*, 4587. [CrossRef]
11. Gautam, L.; Jain, J.K.; Jain, A.; Kalla, P.J.C.; Materials, B. Valorization of bone-china ceramic powder waste along with granite waste in self-compacting concrete. *Constr. Build. Mater.* **2022**, *315*, 125730. [CrossRef]
12. Danish, P.; Ganesh, G.M. Study on influence of Metakaolin and waste marble powder on self-compacting concrete–a state of the art review. *Mater. Today Proc.* **2021**, *44*, 1428–1436. [CrossRef]
13. Aidjouli, Y.; Belebchouche, C.; Hammoudi, A.; Kadri, E.-H.; Zaouai, S.; Czarnecki, S. Modeling the Properties of Sustainable Self-Compacting Concrete Containing Marble and Glass Powder Wastes Using Response Surface Methodology. *Sustainability* **2024**, *16*, 1972. [CrossRef]
14. Rojo-López, G.; González-Fonteboa, B.; Martínez-Abella, F.; González-Taboada, I. Rheology, durability, and mechanical performance of sustainable self-compacting concrete with metakaolin and limestone filler. *Case Stud. Constr. Mater.* **2022**, *17*, e01143. [CrossRef]
15. Zaouai, S.; Tafraoui, A.; Makani, A.; Benmerioul, F. Hardened and transfer properties of self-compacting concretes containing pre-coated rubber aggregates with crushed dune sand. *J. Rubber Res.* **2020**, *23*, 5–12. [CrossRef]
16. Goual, I.; Benabed, B. Mix-design and properties of self-compacting concrete made with calcareous tuff. *J. Build. Eng.* **2020**, *27*, 100997.
17. Najeeb, Z.; Mosaberpanah, M.A. Mechanical and durability properties of modified High-Performance mortar by using cenospheres and Nano-Silica. *Constr. Build. Mater.* **2023**, *362*, 129782. [CrossRef]
18. Environment, U.; Scrivener, K.L.; John, V.M.; Gartner, E.M. Eco-efficient cements: Potential economically viable solutions for a low-CO_2 cement-based materials industry. *Cem. Concr. Res.* **2018**, *114*, 2–26.
19. Habert, G.; De Lacaillerie, J.D.E.; Roussel, N. An environmental evaluation of geopolymer based concrete production: Reviewing current research trends. *J. Clean. Prod.* **2011**, *19*, 1229–1238. [CrossRef]
20. Anderson, D.J.; Smith, S.T.; Au, F.T. Mechanical properties of concrete utilising waste ceramic as coarse aggregate. *Constr. Build. Mater.* **2016**, *117*, 20–28. [CrossRef]
21. Khitas, N.E.H.; Hebbache, K.; Douadi, A.; Boutlikht, M.; Belebchouche, C.; Messai, A.; Mahar, N.E.-H.; Del Serrone, G.; Moretti, L.; Czarnecki, S.J.C.; et al. Modeling and optimizing the properties of mortars based on natural pozzolan, silica sand, and recycled brick waste mixture design: A technical and environmental study. *Constr. Build. Mater.* **2025**, *459*, 139706. [CrossRef]
22. El-Dieb, A.S.; Kanaan, D.M. Ceramic waste powder an alternative cement replacement–Characterization and evaluation. *Sustain. Mater. Technol.* **2018**, *17*, e00063. [CrossRef]
23. Douadi, A.; Hebbache, K.; Boutlikht, M.; Tabchouche, S.; Belebchouche, C.; Hammouche, R.; Del Serrone, G.; Moretti, L. Physical and mechanical effects of silica sand in cement mortars: Experimental and statistical modeling. *Materials* **2023**, *16*, 6861. [CrossRef]
24. Barbhuiya, S.; Nepal, J.; Das, B.B. Properties, compatibility, environmental benefits and future directions of limestone calcined clay cement (LC3) concrete: A review. *J. Build. Eng.* **2023**, *79*, 107794. [CrossRef]
25. Prakash, B.; Saravanan, T.J.; Kabeer, K.S.A.; Bisht, K. Exploring the potential of waste marble powder as a sustainable substitute to cement in cement-based composites: A review. *Constr. Build. Mater.* **2023**, *401*, 132887. [CrossRef]
26. Özkılıç, Y.O.; Zeybek, Ö.; Bahrami, A.; Çelik, A.İ.; Mydin, M.A.O.; Karalar, M.; Hakeem, I.Y.; Roy, K.; Jagadesh, P. Optimum usage of waste marble powder to reduce use of cement toward eco-friendly concrete. *J. Mater. Res. Technol.* **2023**, *25*, 4799–4819. [CrossRef]
27. Soni, A.; Das, P.K.; Hashmi, A.W.; Yusuf, M.; Kamyab, H.; Chelliapan, S. Challenges and opportunities of utilizing municipal solid waste as alternative building materials for sustainable development goals: A review. *Sustain. Chem. Pharm.* **2022**, *27*, 100706. [CrossRef]
28. Wang, D.; Shi, C.; Farzadnia, N.; Shi, Z.; Jia, H.; Ou, Z.J.C.; Materials, B. A review on use of limestone powder in cement-based materials: Mechanism, hydration and microstructures. *Constr. Build. Mater.* **2018**, *181*, 659–672. [CrossRef]
29. Ghezal, A.; Khayat, K.H. Optimizing self-consolidating concrete with limestone filler by using statistical factorial design methods. *Mater. J.* **2002**, *99*, 264–272.

30. Sonebi, M.; Svermova, L.; Bartos, P.J.M. Factorial design of cement slurries containing limestone powder for self-consolidating slurry-infiltrated fiber concrete. *Mater. J.* **2004**, *101*, 136–145.
31. Rizwan, S.A.; Bier, T.A. Blends of limestone powder and fly-ash enhance the response of self-compacting mortars. *Constr. Build. Mater.* **2012**, *27*, 398–403. [CrossRef]
32. Khalid, A.R.; Rizwan, S.A.; Hanif, U.; Hameed, M.H. Effect of mixing time on flowability and slump retention of self-compacting paste system incorporating various secondary raw materials. *Arab. J. Sci. Eng.* **2016**, *41*, 1283–1290. [CrossRef]
33. Felekoğlu, B.; Tosun, K.; Baradan, B.; Altun, A.; Uyulgan, B.J. The effect of fly ash and limestone fillers on the viscosity and compressive strength of self-compacting repair mortars. *Cem. Concr. Res.* **2006**, *36*, 1719–1726. [CrossRef]
34. Rizwan, S.A.; Bier, T.A. Self-consolidating mortars using various secondary raw materials. *ACI Mater. J.* **2009**, *106*, 25. [CrossRef]
35. Belaidi, A.; Azzouz, L.; Kadri, E.; Kenai, S. Effect of natural pozzolana and marble powder on the properties of self-compacting concrete. *Constr. Build. Mater.* **2012**, *31*, 251–257. [CrossRef]
36. Cerquitelli, T.; Pagliari, D.J.; Calimera, A.; Bottaccioli, L.; Patti, E.; Acquaviva, A.; Poncino, M. Manufacturing as a data-driven practice: Methodologies, technologies, and tools. *Proc. IEEE* **2021**, *109*, 399–422. [CrossRef]
37. Hammoudi, A.; Moussaceb, K.; Belebchouche, C.; Dahmoune, F. Comparison of artificial neural network (ANN) and response surface methodology (RSM) prediction in compressive strength of recycled concrete aggregates. *Constr. Build. Mater.* **2019**, *209*, 425–436. [CrossRef]
38. Ali, M.; Macioszek, E. Effect of Pumice Stone as a Coarse Aggregate Replacement on Lightweight Concrete Properties Using Response Surface Methodology. In Proceedings of the International Conference on Computer Methods in Mechanics and 5th Polish Congress of Mechanics, Gliwice, Poland, 4–7 September 2023; pp. 12–26.
39. de Matos, P.R.; Pilar, R.; Bromerchenkel, L.H.; Schankoski, R.A.; Gleize, P.J.; de Brito, J. Self-compacting mortars produced with fine fraction of calcined waste foundry sand (WFS) as alternative filler: Fresh-state, hydration and hardened-state properties. *J. Clean. Prod.* **2020**, *252*, 119871. [CrossRef]
40. Adamu, M.; Trabanpruek, P.; Jongvivatsakul, P.; Likitlersuang, S.; Iwanami, M. Mechanical performance and optimization of high-volume fly ash concrete containing plastic wastes and graphene nanoplatelets using response surface methodology. *Constr. Build. Mater.* **2021**, *308*, 125085. [CrossRef]
41. Adamu, M.; Marouf, M.L.; Ibrahim, Y.E.; Ahmed, O.S.; Alanazi, H.; Marouf, A.L. Modeling and optimization of the mechanical properties of date fiber reinforced concrete containing silica fume using response surface methodology. *Case Stud. Constr. Mater.* **2022**, *17*, e01633. [CrossRef]
42. Li, B.; Chi, Y.; Xu, L.; Shi, Y.; Li, C. Experimental investigation on the flexural behavior of steel-polypropylene hybrid fiber reinforced concrete. *Constr. Build. Mater.* **2018**, *191*, 80–94. [CrossRef]
43. Lalitha, G.; Kumar, S.; Ravali, G.; Santhosh, M.; Dileep, M.J.M. An experimental study on strength parameters of OPC, PPC and geopolymer mortars. *Management* **2022**, *9*, 21–28.
44. Faraj, R.H.; Ahmed, H.U.; Rafiq, S.; Sor, N.H.; Ibrahim, D.F.; Qaidi, S.M. Performance of Self-Compacting mortars modified with Nanoparticles: A systematic review and modeling. *Clean. Mater.* **2022**, *4*, 100086. [CrossRef]
45. Rocha, S.; Ascensão, G.; Maia, L. Exploring Design Optimization of Self-Compacting Mortars with Response Surface Methodology. *Appl. Sci.* **2023**, *13*, 10428. [CrossRef]
46. Goupy, J. *Introduction aux Plans D'expériences*, 1st ed.; Bordas: Paris, France, 2013.
47. Li, L.; Wan, Y.; Chen, S.; Tian, W.; Long, W.; Song, J. Prediction of optimal ranges of mix ratio of self-compacting mortars (SCMs) based on response surface method (RSM). *Constr. Build. Mater.* **2022**, *319*, 126043. [CrossRef]
48. Ghrici, M.; Kenai, S.; Said-Mansour, M. Mechanical properties and durability of mortar and concrete containing natural pozzolana and limestone blended cements. *Cem. Concr. Compos.* **2007**, *29*, 542–549. [CrossRef]
49. Shah, V.; Parashar, A.; Mishra, G.; Medepalli, S.; Krishnan, S.; Bishnoi, S. Influence of cement replacement by limestone calcined clay pozzolan on the engineering properties of mortar and concrete. *Adv. Cem. Res.* **2020**, *32*, 101–111. [CrossRef]
50. Benkaddour, M.; Kenai, S.; Yahiaoui, W.; Bensaci, H.; Khatib, J. Rheological, mechanical and durability performance of some North African commercial binary and ternary cements. *Case Stud. Constr. Mater.* **2023**, *19*, e02689. [CrossRef]
51. *EN 197-1:2011*; Cement—Part 1: Composition, Specifications and Conformity Criteria for Common Cements. iTeh Standards: Etobicoke, ON, Canada, 2011.
52. Moulay-Ali, A.; Abdeldjalil, M.; Khelafi, H. An experimental study on the optimal compositions of ordinary concrete based on corrected dune sand—Case of granular range of 25 mm. *Case Stud. Constr. Mater.* **2021**, *14*, e00521. [CrossRef]
53. Okamura, H.; Ozawa, K.; Ouchi, M. Self-compacting concrete. *Struct. Concr.* **2000**, *1*, 3–17. [CrossRef]
54. *ASTM C1585*; Standard Test Method for Measurement of Rate of Absorption of Water by Hydraulic-Cement Concretes. ASTM International: West Conshohocken, PA, USA, 2013; Volume 41, pp. 1–6.
55. *EN 1015-11*; Methods of Test for Mortar for Masonry—Part 11: Determination of Flexural and Compressive Strength of Hardened Mortar. iTeh Standards: Etobicoke, ON, Canada, 2019.

56. *C1403–13*; Standard Test Method for Rate of Water Absorption of Masonry Mortars1. ASTM International: West Conshohocken, PA, USA, 2015.
57. Raju, M.R.; Ahmad, S.I.; Hasan, M.M.; Hasan, N.M.S.; Islam, M.M.; Basit, M.A.; Hossain, I.T.; Santo, S.A.; Alam, M.S.; Rahman, M. Machine learning for predicting strength properties of waste iron slag concrete. *Heliyon* **2025**, *11*, e42133. [CrossRef]
58. Pelánek, R. Metrics for Evaluation of Student Models. *J. Educ. Data Min.* **2015**, *7*, 1–19.
59. Hammouche, R.; Belebchouche, C.; Hammoudi, A.; Douadi, A.; Czarnecki, S.J.J.o.C.P. Modeling and Optimizing the Durability of Self-Compacting Mortars Incorporating Cement Kiln Dust and Glass Powder: A Box-Behnken Design Study. *J. Clean. Prod.* **2025**, *502*, 145282. [CrossRef]
60. Liu, C.; Li, Z.; Bezuijen, A.; Chen, L.; Cachim, P. Optimizing the shield tunnel backfilling grouts with supplementary cementitious materials by response surface methodology. *Constr. Build. Mater.* **2024**, *421*, 135575. [CrossRef]
61. Badaoui, M.; Hebbache, K.; Douadi, A.; Mansouri, L.; Merdas, A.; Gherbi, S.; Kada, K.; Boutlikht, M.; Belebchouche, C.; Szymanowski, J. Utilization of Algerian calcined clay in sustainable mortars considering thermal treatment and granulometry effects on mechanical properties. *Sci. Rep.* **2025**, *15*, 21704. [CrossRef]
62. Belkadi, A.A.; Kessal, O.; Berkouche, A.; Noui, A.; Daguiani, S.E.; Dridi, M.; Benaniba, S.; Tayebi, T. Experimental investigation into the potential of recycled concrete and waste glass powders for improving the sustainability and performance of cement mortars properties. *Sustain. Energy Technol. Assess.* **2024**, *64*, 103710.
63. Yahia, A.; Tanimura, M.; Shimoyama, Y. Rheological properties of highly flowable mortar containing limestone filler-effect of powder content and W/C ratio. *Cem. Concr. Res.* **2005**, *35*, 532–539. [CrossRef]
64. Belouadah, M.; Rahmouni, Z.E.; Tebbal, N.; Hicham, M.E.H. Evaluation of Concretes Made with Marble Waste Using Destructive and Non-Destructive Testing. *Ann. Chim. Sci. Matériaux* **2021**, *45*, 361–368. [CrossRef]
65. Chen, H.; Feng, P.; Du, Y.; Jiang, J.; Sun, W. The effect of superhydrophobic nano-silica particles on the transport and mechanical properties of hardened cement pastes. *Constr. Build. Mater.* **2018**, *182*, 620–628. [CrossRef]
66. Oltulu, M.; Şahin, R. Pore structure analysis of hardened cement mortars containing silica fume and different nano-powders. *Constr. Build. Mater.* **2014**, *53*, 658–664. [CrossRef]
67. Lanzón, M.; García-Ruiz, P. Evaluation of capillary water absorption in rendering mortars made with powdered waterproofing additives. *Constr. Build. Mater.* **2009**, *23*, 3287–3291. [CrossRef]
68. Benli, A. Mechanical and durability properties of self-compacting mortars containing binary and ternary mixes of fly ash and silica fume. *Struct. Concr.* **2019**, *20*, 1096–1108. [CrossRef]
69. Olivier, J.G.; Schure, K.; Peters, J.A.H.W. *Trends in Global CO_2 and Total Greenhouse Gas Emissions*; PBL Netherlands Environmental Assessment Agency: The Hague, The Netherlands, 2017; Volume 5, pp. 1–11.
70. Makhlouf, A.; Kardache, R.; Chaabia, R.; Drouiche, A.; Brahmi, B. Environmental Impact Assessment of the Algerian Cement Industry: A Case Study with Life Cycle Assessment Methodology. In *Selected Studies in Environmental Geosciences and Hydrogeosciences*; Springer: Cham, Switzerland, 2020; pp. 83–85.
71. Singh, A.; Thakare, A.A.; Chaudhary, S. A case study on examining the fresh-state behavior of self-compacting mortar containing waste powders from various sources. *Case Stud. Constr. Mater.* **2023**, *19*, e02684. [CrossRef]
72. Souza, A.T.; Barbosa, T.F.; Riccio, L.A.; dos Santos, W.J. Effect of limestone powder substitution on mechanical properties and durability of slender precast components of structural mortar. *J. Mater. Res. Technol.* **2020**, *9*, 847–856. [CrossRef]
73. Faheem, A.; Rizwan, S.A.; Bier, T.A. Properties of self-compacting mortars using blends of limestone powder, fly ash, and zeolite powder. *Constr. Build. Mater.* **2021**, *286*, 122788. [CrossRef]
74. Ezziane, K.; Kadri, E.; Hallal, A.; Duval, R. Effect of mineral additives on the setting of blended cement by the maturity method. *Mater. Struct.* **2010**, *43*, 393–401. [CrossRef]
75. Türkel, S.; Altuntaş, Y. The effect of limestone powder, fly ash and silica fume on the properties of self-compacting repair mortars. *Sadhana* **2009**, *34*, 331–343. [CrossRef]
76. Gürol, G. Components for Economic Concrete, cement/water/fine and coarse aggregate/chemical and mineral admixtures. *J. Des. Constr.* **1999**, *164*, 66–74.
77. Güneyisi, E.; Gesoğlu, M. Properties of self-compacting mortars with binary and ternary cementitious blends of fly ash and metakaolin. *Mater. Struct.* **2008**, *41*, 1519–1531. [CrossRef]
78. Safiuddin, M.; West, J.; Soudki, K. Hardened properties of self-consolidating high performance concrete including rice husk ash. *Cem. Concr. Compos.* **2010**, *32*, 708–717. [CrossRef]
79. Sua-Iam, G.; Makul, N. Utilization of limestone powder to improve the properties of self-compacting concrete incorporating high volumes of untreated rice husk ash as fine aggregate. *Constr. Build. Mater.* **2013**, *38*, 455–464. [CrossRef]
80. Şahmaran, M.; Christianto, H.A.; Yaman, İ.Ö. The effect of chemical admixtures and mineral additives on the properties of self-compacting mortars. *Cem. Concr. Compos.* **2006**, *28*, 432–440. [CrossRef]
81. Bonavetti, V.; Donza, H.; Menendez, G.; Cabrera, O.; Irassar, E. Limestone filler cement in low w/c concrete: A rational use of energy. *Cem. Concr. Res.* **2003**, *33*, 865–871. [CrossRef]

82. Péra, J.; Husson, S.; Guilhot, B. Influence of finely ground limestone on cement hydration. *Cem. Concr. Compos.* **1999**, *21*, 99–105. [CrossRef]
83. Toubal Seghir, N.; Mellas, M.; Sadowski, Ł.; Krolicka, A.; Żak, A. The Effect of Curing Conditions on the Properties of Cement-Based Composites Blended with Waste Marble Dust: Toubal Seghir, Mellas, Sadowski, Krolicka, and Żak. *JOM* **2019**, *71*, 1002–1015. [CrossRef]
84. Çakır, Ö.; Aköz, F. Effect of curing conditions on the mortars with and without GGBFS. *Constr. Build. Mater.* **2008**, *22*, 308–314. [CrossRef]